TAPHONOMY OF THE SUN RIVER BONEBED, LATE CRETACEOUS (CAMPANIAN) TWO MEDICINE FORMATION OF MONTANA

by

Benjamin Andrew Scherzer

A thesis submitted in partial fulfillment
of the requirements for the degree

of

Master of Science

in

Earth Sciences

MONTANA STATE UNIVERSITY-BOZEMAN
Bozeman, Montana

April 2008

APPROVAL

of a thesis submitted by

Benjamin Andrew Scherzer

This thesis has been read by each member of the thesis committee and has been found to be satisfactory regarding content, English usage, format, citations, bibliographic style, and consistency, and is ready for submission to the Division of Graduate Education.

Dr. David J. Varricchio

Approved for the Department of Earth Sciences

Dr. Stephan G. Custer

Approved for the Division of Graduate Education

Dr. Carl A. Fox

STATEMENT OF PERMISSION TO USE

Benjamin Andrew Scherzer

April 2008

ACKNOWLEDGEMENTS

This thesis would not have come to completion without the help of each member of my committee: Dave Varricchio, Jack Horner, and Jim Schmitt. Field work would have been impossible if not for the work of my field assistants: Josh Bonde, Pete Bucholz, Jennifer Krey, John Plummer, Anne Teppo, and Eric Williams. The Museum of the Rockies was generous in both providing me office space and sharing field equipment. Additional academic assistance came from Mic Jackson (Earlham College), Anthony Martin (Emory University), Greg Retallack (University of Oregon), Eric Roberts (Southern Utah University). Finally, my family, as always, was patient, supportive, and occasionally blunt.

Field work was possible thanks to permission from the State of Montana and the BLM. This project was funded by the Jurassic Foundation and The American Museum of Natural History's Theodore Roosevelt Memorial Fund.

IN MEMORIAM, 1988-2004

TABLE OF CONTENTS

TABLE OF CONTENTS – CONTINUED

LIST OF TABLES

Table Page

LIST OF FIGURES

LIST OF FIGURES – CONTINUED

LIST OF FIGURES – CONTINUED

Figure Page

ABSTRACT

In the summer of 1998, a bonebed of juvenile dinosaur material was found in beds of the Two Medicine Formation along the Sun River in Teton County, Montana. Initial inspection of the "Sun River Bonebed" indicated unique dominance by juvenile remains and unusually high concentration of fossil material. Modern exposure of both the bonebed and surrounding strata allowed for a detailed taphonomic study of the assemblage.

In the summer of 2004, the bonebed was excavated in a fashion that recorded depthwise taphonomic data of fossil material and surrounding sediment, and allowed for three-dimensional reconstruction of the bonebed. The lithology of the surrounding beds was documented for 120 m immediately below and 40 m immediately above the bonebed to interpret the overall depositional environment of the area. Lastly, the paleobiologic and sedimentologic interpretations made for the bonebed were compared to bonebeds of similar fauna in the Two Medicine Formation.

Taphonomic attributes of the fossil material indicate a mass death assemblage of late juvenile lambeosaurines subject to post-mortem bioturbation and possible fluvial transport. A number of elements from the assemblage exhibit a rare form of taphonomic modification known as "wet rot," currently documented in only one other dinosaur bonebed. Sedimentologic and additional taphonomic data in the assemblage indicate entrainment of the vertebrate material in a cohesive debris flow and ultimate deposition in the respective flow deposit. The sedimentology of the surrounding beds indicates ultimate deposition in an ephemeral fluvial environment. The restricted age class representation of the assemblage lends credence to existing paleobiologic interpretations of hadrosaurids in the Late Cretaceous of Montana, and the Sun River Bonebed is significant in its exhibition of "wet rot" modification and in being one of a restricted number of documented debris-flow hosted vertebrate bonebeds.

CHAPTER 1

INTRODUCTION

The incorporation of taphonomy into the field of vertebrate paleontology has ushered exceptional growth in the understanding of the geologic and biologic history of fossil localities and their fauna. Fossilization of vertebrate material can occur under a variety of conditions (see Behrensmeyer and Hook, 1992), ranging from numerous fluvial, lacustrine, and floodplain deposits, to material preserved in volcanic ash falls (Voorhies, 1985), subaqueous microbial mats (Briggs et al., 1997), hot springs (Channing et al., 2004), tar pits (Stock, 1956), karst ponds (Agenbroad, 1984), and even scatological deposits (Mellett, 1974). Detailed taphonomic examination of vertebrate bonebeds permits significant paleobiologic interpretations, including social structure (Berger et al., 2001), specific carnivore activity (Haynes, 1980; 1983b; Blumenschine and Marean, 1993), nesting behavior (Meng et al., 2004), and even diet (Chin et al., 1998). However, since there are rarely specific, unique taphonomic signatures common to particular depositional settings, a detailed taphonomic evaluation of a fossil deposit must maintain a multidisciplinary focus, assimilating data from sedimentologic and paleobiologic perspectives.

The Late Cretaceous Two Medicine Formation of Montana is a particularly valuable resource for taphonomic information for a number of reasons. The Two Medicine was deposited within a foreland basin, a basin type considered the “major loci of preservable nonmarine sedimentation” (DeCelles, 1986, p. 912), which commonly preserves a uniquely abundant and extensive vertebrate fossil record (Rogers, 1993). The Two Medicine, in particular, also contains diverse fossil accumulations, ranging from petrified forests (Roberts and Hendrix, 2000; Falcon-Lang, 2003), to widespread lag deposits (Rogers and Kidwell, 2000), to ceratopsian and hadrosaurid bonebeds "unsurpassed in size and abundance" (Varricchio, 1995, p. 298). In addition, the impressive fossil record is also combined with an excellent chronostratigraphic record, with sedimentation influenced by several sea level cycles, allowing for the application of nonmarine sequence stratigraphy (Rogers, 1998; Roberts, 1999). This allows for unique examination of the processes of sea level fluctuation, environmental change, and dinosaur evolution within the same formation (Horner, 1984; Horner et al., 1992).

In 1998, fossil dinosaur material was found in the Two Medicine Formation along the Sun River in Teton County between Choteau and Augusta, Montana. Brief inspection of the bonebed indicated it was unique in both its high density of bones (bones/m^2) compared to other Two Medicine bonebeds, and its apparent domination by juvenile hadrosaurid elements, a particularly rare age composition in the fossil record (Fiorillo, 1991). Finally, due to its location along the Sun River, strata of the Two Medicine Formation, including the bonebed, were well exposed. As a result, the opportunity was available for a detailed taphonomic study of the Sun River Bonebed (SRB).

The goals of this project were threefold, and were divided between sedimentology, taphonomy, and paleobiology. Sedimentologically, it was necessary to determine the lithology and depositional environment of the local beds, including the Sun River Bonebed. Taphonomically, this project was focused on how the sedimentologic and biologic environment were responsible for the taphonomic modification of the fossil assemblage, and what the assemblage could indicate about possible causes of death. The taphonomic interpretations could then be compared to other hadrosaurid bonebeds in the Two Medicine Formation, leading to possible paleobiologic implications for hadrosaurids in the Late Cretaceous of Montana.

CHAPTER 2

LOCATION AND GEOLOGIC SETTING

The Sun River Bonebed (SRB) is located on State of Montana land along the Sun River at the southern border of Teton County, approximately 37 km southwest of Choteau, Montana (Fig. 1). The Two Medicine Formation in this area is steeply dipping, with strata containing the SRB dipping approximately 45º. The Sun River has cut down through the beds, producing an approximately 4.5 km long stretch of intermittently exposed strata, predominantly on the north side of the river.

In the Late Cretaceous of Montana, sediment shed from the rocks exposed in the Cordilleran thrust belt (Gill and Cobban, 1973), and volcanics from the Elkhorn Mountains volcanic field (Lorenz and Gavin, 1984) and possibly the Adel Mountains (Smith, 1998), formed two major clastic wedges extending eastward into the Cretaceous Western Interior Seaway (Gill and Cobban, 1973). The Two Medicine Formation was the portion of the sediment deposited proximal to the thrust belt (Kauffman, 1977; Lorenz and Gavin, 1984). The Two Medicine abruptly overlies the Campanian Virgelle Sandstone, with the contact commonly demarcated by a thin coal layer, and is abruptly overlain in most areas by the Campanian-Maastrichtian Bearpaw Shale, with some areas showing a transition into the overlying Campanian-Maastrichtian Horsethie and St. Mary formations (Lorenz and Gavin, 1984). The rocks of the upper ~500 m of the Two Medicine Formation are syndepositional with the eastern, distal portion of the clastic wedge, the Judith River Formation (Lorenz and Gavin, 1984). Exposed Two Medicine

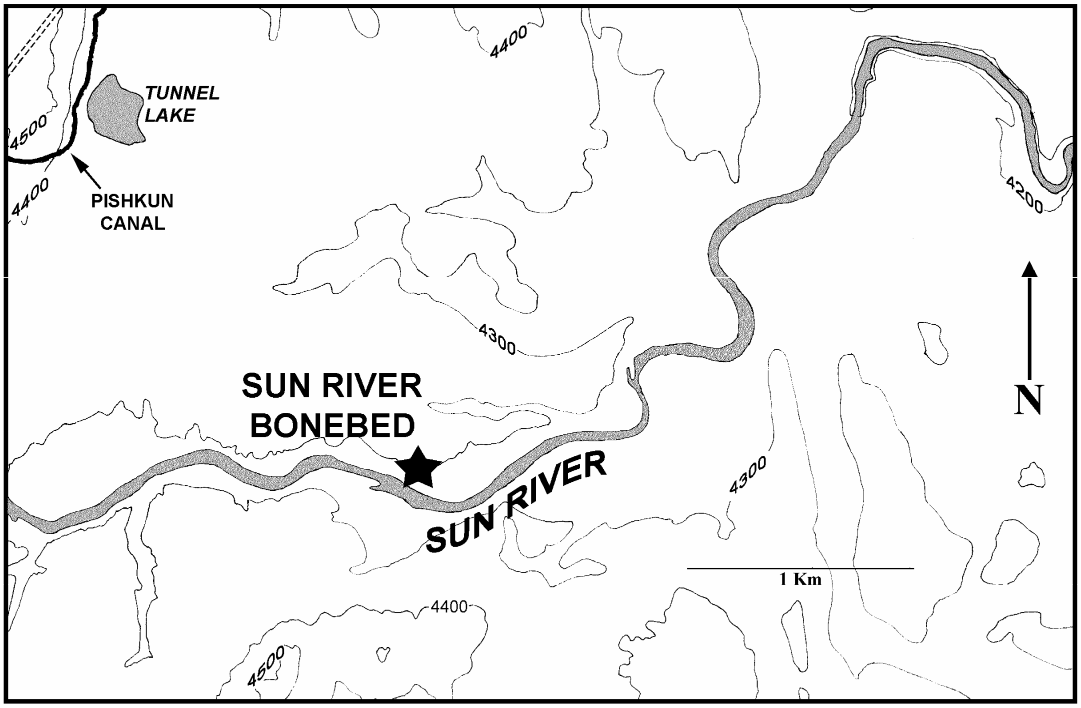

Figure 1: Location of the Sun River Bonebed in Teton (north of Sun River) and Lewis and Clark Counties (south of Sun River), Montana (Teton Co: T 22 N, R 8 W).

and Judith River beds are separated by the post-Cretaceous Sweetgrass arch (Rogers, 1998). Radiometric dates of bentonitic beds in the Two Medicine Formation range from ~80 to 74 Ma (Rogers et al., 1993).

The ratio of beds of fines (claystone-siltstone) to sandy beds is higher in the Two Medicine than in the Judith River, with beds of fines commonly displaying evidence of pedogenesis (Rogers, 1993). Varricchio (1995) provides a summary of evidence indicating the environment of the Two Medicine Formation as transitory between warm, tropical southern evergreen forests, and temperate, northern deciduous forests. The SRB is located within the Disturbed Belt, a zone of numerous imbricate thrust faults, approximately 65 miles long (N-S) and 20 miles wide (E-W) along the westernmost extent of the Two Medicine along the Rocky Mountain Front (Woodward, 1981).

Within the 4.5 km stretch of intermittently exposed strata along the Sun River, the SRB is present in a 160 m long exposure. Due to the steep dip of the beds, lateral exposure is truncated by erosion and covered by Pleistocene glacial till. The outcrop is dominated by mudrock and fine to medium-grained sandstone. Isolated vertebrate material occurs within both sandstone and mudstone, and a tightly associated *Daspletosaurus* specimen (MOR 1130) was excavated from a nearby sandstone by a Museum of the Rockies crew in 2001.

CHAPTER 3

METHODS

Excavation of the SRB in the summer of 2004 included 3D mapping, in situ inspection of bone surfaces, screening for microvertebrate and invertebrate fossils, collection of coalified plant fossils and calcareous clasts, and monitoring of grain size and color of matrix. Specimens were extracted from the matrix using awls, dental picks, and brushes. Approximately 0.15 m^3 of matrix (almost $1/3^{rd}$ of total matrix volume) was washed and screened at the beginning of excavation to check for microvertebrate and invertebrate fossil material. After this screening produced no additional material, this process was abandoned. Weathering was assessed using the stages of Fiorillo (1988b), abrasion was assessed using the stages of Shipman (1981, p. 114), and fracturing patterns were largely classified based on Haynes (1983a) (modification to fracturing patterns will be discussed later in *WEATHERING AND ABRASION*).

Bone surfaces were inspected during excavation for evidence of weathering, abrasion, and other taphonomic indicators such as tooth marks or crushing. The upside of each element, its completeness, and its immediately surrounding matrix were also recorded during excavation. An effort was made to collect all bones and bone fragments, as well as other material such as calcareous clasts or coalified plant fossils. Following lab preparation, bone modification of elements was reexamined. Several calcareous clasts of varying size were also manually broken, and examined with a binocular microscope to investigate internal structure.

Bones were mapped in 3D, relative to the bedding plane, using the serial section method designed by Abler (1984). The bed was excavated in 5 cm depth intervals, mapping the exposed portions of bones using a meter grid subdivided into 10-cm partitions (Fig. 2). An effort was made to maintain an excavation surface parallel to the bedding plane, with the orientation of the excavation surface consistently monitored with a Brunton compass. Following full excavation of all meter grids, the individual maps were then combined to produce a three-dimensional map view of the bonebed (Appendix A). Orientation of elongate elements was also measured using a Brunton compass. Trends and plunges of elongate elements were plotted using *Stereonet for Windows* (Allmendinger, 2002). All orientation data were palinspastically restored.

Matrix grain size and color were evaluated, and matrix samples were also collected, for each 5-cm depth interval. Samples of the beds underlying and overlying the bonebed were collected as close to the respective contact as possible. Following excavation, matrix and rock samples were soaked in water until visibly disaggregated, and wet screened with U.S. Standard Sieves down to a 2 mm (-1 φ) – 0.25 mm (2 φ) size. This sieving procedure removed large particles (modern root fragments, small calcareous clasts) and loose fine particles (loose silt - clay) to allow for examination of the sediment with a standard binocular microscope. A detailed section through the bonebed was produced following excavation by combining data gathered at each 5 cm depth interval.

The SRB was excavated by Museum of the Rockies crews in 2000, 2001, and 2004. Previous excavations of the SRB include brief surficial collection in the summer of 2000 and shallow quarrying and unscaled mapping in the summer of 2001. Taphonomic

Figure 2: Exposed bones parallel to bedding in the SRB, within a marked partial 1 m^2 grid. Two sides of grid are delineated by string, a third partially so. Grid boundaries commonly extended into overlying outwash. North arrow not pointing north.

data, sedimentologic description, bone orientation, and depthwise data were not collected in the two previous excavations. Quarry maps were produced for material excavated in the summer of 2001, but were not included in the composite bonebed map for the 2004 excavation. Previously excavated and prepared material was included in bone counts and assessed for bone modification, but were not included in data sets otherwise. All SRB specimens are curated at the Museum of the Rockies collections in Bozeman, Montana under specimen number MOR 1142, locality TM-260.

A stratigraphic section of the study area was measured using a Jacob staff and Brunton compass. Beds were followed laterally in the field to document changes in thickness, grain size, sedimentary structures, or lateral transition into other beds. Lithofacies were based on grain size, texture, sedimentary structures, and grading, and classified using the terminology of Miall (2006, p. 79) and Eberth and Miall (1991).

CHAPTER 4

LITHOFACIES

Approximately 160 m of continuously exposed Two Medicine Formation strata are present along the Sun River in the area of SRB, with the bonebed stratigraphically located approximately 120 m from the base (Appendix B). The Two Medicine Formation in the study area is dominated by mudrock (mudstone-siltstone) and sandstone. Mudrocks are exclusively massive (Fm). Sandstone beds are predominantly massive (Sm), with trough cross-bedded sandstone (St) and horizontally bedded sandstone (Sh) common. A matrix-supported massive conglomerate (Gmm) and two discrete bentonite horizons (Fb) are also present. Summaries of lithofacies are given in Table 1. Locations of beds shown in figures are denoted in Appendix B.

Matrix-Supported Massive Conglomerate (Gmm)

Description

This facies (Fig. 3) is present as a 0.65 m bed composed of clasts (0.5–2 cm) of mudstone, caliche, and chert supported in a matrix of muddy coarse grained sand. No grading or imbrication of clasts was observed, and clasts are evenly distributed vertically. The lower contact of the bed is abrupt and uneven; the underlying bed is highly eroded and covered with vegetation and rock fragments from other beds. Contact with the overlying trough cross-stratified sandstone (St) is abrupt and uneven, with mud rip-up clasts present at the base. Lateral exposure is sporadic for ~50 m, the eroded nature of the

Table 1: Lithofacies of the Two Medicine Formation in the study area. Facies codes based on Miall (2006, p. 79) and Eberth and Miall (1991).

	Lithofacies	Description	Interpretation
Gmm	Matrix-supported massive conglomerate	Occurs as a 0.65 m bed. Contacts with overlying trough cross-bedded sandstone (St) and underlying bed abrupt.	Lag deposit
St	Trough cross-bedded sandstone	Occur as cosets (3-5 m). Contacts with overlying beds abrupt, contact with underlying beds can be abrupt or gradational.	3D dunes in lower flow regime
Sr	Ripple cross-laminated sandstone	Occurs as a 0.2 m bed. Contacts with underlying trough cross-bedded sandstone and overlying bed obscured.	Lower flow regime, ripples
Sh	Horizontally bedded sandstone	Thick beds (1.5-2 m). Contacts with overlying and underlying beds abrupt when visible.	High velocity deposition in transition from lower to upper flow regime; Low velocity deposition in lower flow regime
Sm	Massive sandstone	Ungraded sandstone beds ranging from 1 to 8 m in thickness. Contact with overlying and underlying beds can be abrupt or gradational. Often interbedded with thin (0.05-0.2 m) mudrock beds (Fm).	Various: rapid deposition during flooding, bank collapse, hyper-concentrated flow, bioturbation, soft-sediment deformation
Fm	Massive mudrock	Massive siltstone-claystone beds 0.05 to >10 m in thickness. Contact with overlying and underlying beds can be abrupt or gradational. Thin (<0.3 m) beds often interbedded with massive sandstone (Sm), thicker (~0.5 m) beds often grade out of massive sandstone (Sm).	Suspension settling in standing water
Fb	Bentonite	Massive beds (2-3 m) of ash to lapilli. Contacts with overlying beds gradational, contacts with underlying beds very sharp.	Volcaniclastic ash fall

Figure 3: Matrix-supported massive conglomerate (Gmm) underlying a sandstone bed.

bed obscures any lateral change in thickness.

Interpretation

Massive, ungraded, matrix-supported conglomerates are typically interpreted to represent deposits of debris flows (e.g. Shultz, 1984; Miall, 2006, p. 106), however, such lithofacies can also represent lags at the base of individual flood deposits on floodplains and in channels (Stear, 1985; Miall, 2006, p. 93). The overlying trough cross-bedded sandstone suggests this conglomerate was a lag deposit moved at peak flood time (Walker and Cant, 1984), though the sharp, uneven upper contact and rip-up clasts at the base of the overlying trough cross-bedded sandstone (St) indicate a sedimentation break, and possible exposure and erosion, prior to subsequent, lower-energy deposition in the flood. The massive, ungraded, matrix-supported texture also indicates that, in contrast to the bipartite deposition of clasts and matrix in clast-supported conglomerates (Miall, 2006, p. 101), the clasts and matrix of this conglomerate were deposited simultaneously.

Trough Cross-Bedded Sandstone (St)

Description

Trough cross-bedded sandstone (Fig. 4) is commonly coarse grained, but can be medium grained as well. These facies occur exclusively as 3-5 m thick cosets; the number of individual sets per coset were not counted. Contacts with overlying beds are abrupt; contacts with underlying beds can be abrupt or gradational. Mud rip-up clasts are present at the base of most cosets, with mud rip-up clasts also common at the base of individual sets (Fig. 5). Unidentified invertebrate trace fossils are occasionally present at the base of cosets (Fig. 6), as well as one lag deposit of disarticulated *Unio* shells. A concentration of fragmentary plant material is also present at the base of one set. Several beds extend laterally for 30 – 50 m, one bed for over 100 m; no beds show any lateral change in thickness, grain size, or sedimentary structures.

Interpretation

Trough cross-bedded sands are interpreted to represent preserved migration of 3D dunes (Miall, 1977). The tabular geometry of the beds, abundance of mud rip-up clasts,

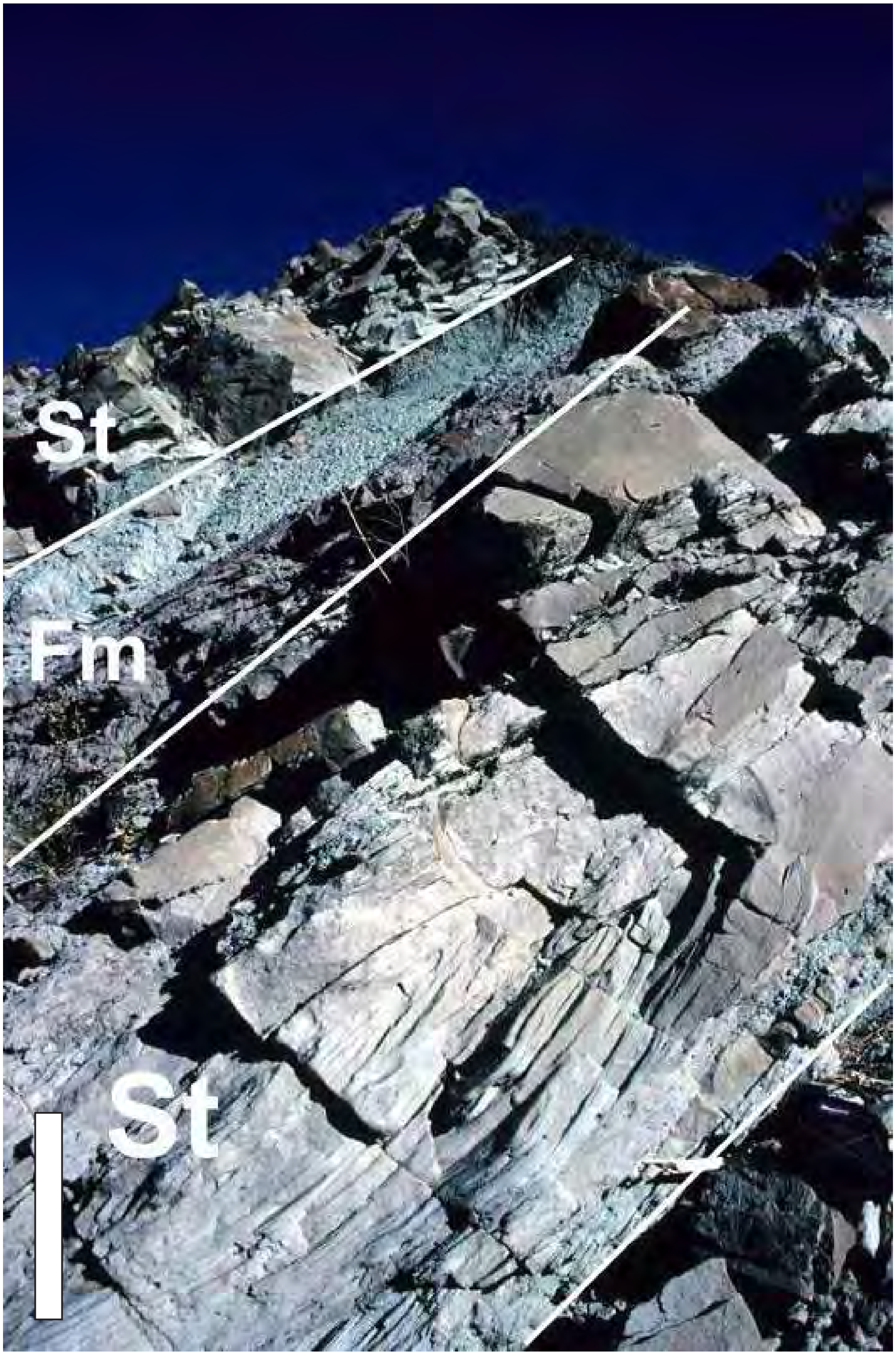

Figure 4: Typical exposure of trough cross-bedded sandstone (St). Scale bar is 1 m.

Figure 5: Mud rip-up clasts at the base of a set in trough cross-bedded sandstone (St).

Figure 6: Unidentified trace fossils at the base of a trough cross-bedded sandstone (St).

abrupt lower contacts (Eberth et al., 2000), presence of plant fragments (Tunbridge, 1981), and freshwater invertebrate fossils, and absence of marine invertebrate fossils, all suggest a fluvial origin for this facies, with dunes forming under lower flow regime velocities (Harms and Fahnestock, 1965; Harms et al., 1975).

Ripple Cross-Laminated Sandstone (Sr)

Description

Ripple cross-laminated sandstone is medium to coarse grained, and occurs in one 0.2 m bed that contains interference ripple form sets on its upper surface (Fig. 7). Contacts with the underlying trough cross-bedded sandstone and overlying bed are obscured by erosion and heavy vegetation, as is lateral exposure.

Interpretation

This facies is interpreted to represent preservation of migrating ripples (Harms et al., 1975; Miall, 1977). Interference ripples result from interaction of multiple waves or currents flowing in different directions (Collinson and Thompson, 1982, p. 71).

Horizontally Laminated Sandstone (Sh)

Description

Horizontally laminated sandstone (Fig. 8) is commonly fine to medium grained, occasionally becoming coarse-grained. Beds are commonly thick (1.5-3 m), and contacts with overlying and underlying beds are abrupt when visible. Individual laminae are 0.2 – 1 cm in thickness.

Figure 7: Upper bedding surface of ripple cross-laminated sandstone (Sr) showing interference ripple form sets. North arrow is 10 cm long.

Figure 8: Exposure of horizontally laminated sandstone (Sh).

Thinner (0.5 m) beds are also present interbedded with massive mudrock (Fm) in one exposure, with abrupt upper and lower contacts, and mudcrack casts and concavities from eroded mud rip-up clasts visible on the lower contacts (Fig. 9). In the same exposure, numerous ovoid to sub-circular, unpaired, straight-edged, mud-filled “holes” were seen extending through several sandstone beds (Fig. 10), interpreted to be insect burrows of the *Coprinisphaera* ichnofacies (Genise et al., 2000).

Many of the horizontally laminated sandstones (Sh) show convoluted laminae, composed of regularly to irregularly spaced folds within a bed (Fig. 11). The intensity of the deformation varies, with some beds showing relatively shallow folds that die out with depth, and other beds showing intense, overturned folds throughout their thickness. Beds

Figure 9: Mudcrack casts and concavities from eroded mud rip-up clasts at the base of a horizontally bedded sandstone (Sh).

Figure 10: Ovoid to sub-circular holes seen from the upper bedding surface in horizontally laminated sandtones (Sh).

Figure 11: Convolute laminae near the base of a horizontally laminated sandstone (Sh).

are rarely exposed laterally for more than 20 m, with no lateral change in thickness, grain size, or sedimentary structure observed.

Interpretation

Horizontally laminated sand can be deposited both in very low flow regime conditions and in upper flow regime conditions (Miall, 2006, p. 115-120). The common fine to medium grain size suggests this facies was most commonly deposited under upper flow regime conditions (Stear, 1985; Fedo and Cooper, 1990; Miall, 2006, p. 120); when interbedded with massive mudrock (Fm), however, this facies is interpreted to represent deposition under very low flow velocities (Leeder, 1999, p. 150; Miall, 2006, p. 120). The occurrence of convolute laminae could have resulted from vertical dewatering due to rapid deposition (Allen, 1977; Tunbridge, 1981), or also from bioturbation during subaerial exposure of beds following flooding events.

Massive Sandstone (Sm)

Description

Massive sandstone (Sm) is fine to coarse grained. Individual beds range from 0.1 to 8 m in thickness. Contacts with overlying and underlying beds can be abrupt or gradational. Thinner beds (<0.3 m) of this facies are interbedded with thin (<0.2 m) beds of massive mudrock (Fm) commonly showing unidentified trace fossils on lower contacts (Fig. 12). Less commonly this facies fines upward into thicker (>0.5 m) mudrock (Fm), or grades out of mudrock (Fm). Abrupt contacts with underlying massive mudrock (Fm) occasionally show load casts and the upper contact of a massive sandstone underlying the SRB shows signs of bioturbation (Fig. 13). The associated remains of an adult *Daspletosaurus* (MOR 1130), separate from the SRB, were excavated from a bed characterized by this facies in 2001. Beds are commonly exposed laterally for less than 20–30 m, but two massive sandstone (Sm) beds extend for up to 100 m. No lateral change in thickness, grain size, or sedimentary structure occurs in any bed.

Interpretation

Massive sandstones could result from several conditions, such as rapid deposition during flooding events (Collinson, 1969; McCabe, 1977), bank collapse and liquification (Jones and Rust, 1983; Rust and Jones, 1987; Turner and Munro, 1987; Wizevich, 1992),

Figure 12: Lower bedding surface of massive sandstone (Sm) interbedded with massive mudrock (Fm), showing unidentified trace fossils.

Figure 13: Bioturbated upper contact of massive sandstone (Sm) underlying the SRB.

or hyperconcentrated flow (G. A. Smith, 1986). These conditions would have resulted in rapid deposition of suspended sand lacking in any bedform structures (G. A. Smith, 1986). Massive sands could also have resulted from intense bioturbation following deposition; considering the indication of bioturbation seen in horizontally laminated sandstones (Sh), this is a likely possibility.

Massive Mudrock (Fm)

Description

This facies consists of massive unlaminated mudstone and siltstone, ranging from 0.5 to more than 10 m in thickness (Fig. 14). No evidence of root traces, bioturbation, or invertebrate fossils was found, largely due to the swelling and “popcorn” weathering typical of Two Medicine mudstones (Lorenz, 1981). Contacts with overlying beds can be abrupt or gradational. Thin beds (<0.3 m) are typically interbedded with massive sandstone (Sm), and thicker (0.5-2.5 m) beds occasionally grade out of massive sandstone (Sm). Abrupt contacts with overlying massive sandstone (Sm) and trough cross-bedded sandstones (St) are often swaley, and occasionally contain various unidentified invertebrate trace fossils. Bone float was also suspected to have originated from the base of a massive mudrock (Fm) approximately 15 m above SRB. Two bentonite horizons (Fb) are present within this facies, with sharp contacts below and gradational contacts above. Colors vary widely within beds, and include red, purple, green, blue, brown, and grey. Lateral exposure of massive mudrock (Fm) beds varies, and is dictated almost entirely by the lateral exposure of more resistant overlying and/or underlying sandstone beds. No lateral change in thickness, grain size, or sedimentary structure was observed in any massive mudrock (Fm), even in the most laterally exposed (50^{+} m) beds.

Figure 14: Exposure of massive mudrock (Fm).

Interpretation

This facies is interpreted to represent vertical accretion by settling of fines from suspension (Miall, 1977). The lack of freshwater or marine fossils (Scott, 1978; Fielding, 1984; Haszeldine, 1984) or fine lamination (Larsen and Crossey, 1996) along with the presence of mud cracks and mud rip-up clasts in overlying trough cross-bedded sandstones (St) and horizontally laminated sandstones (Sh), suggest subaerial exposure of the fines following deposition. Color variation within beds could also indicate pedogenesis (Platt and Keller, 1992). Massive mudrocks (Fm) interbedded with massive sandstone (Sm) could represent deposition during fluctuating water levels (Jackson, 1978; Eberth, 1993). The presence of red and purple mudstones in the study area places the Sun River Bonebed in the upper lithofacies of the Two Medicine Formation (Lorenz, 1981), an interpretation that agrees with unpublished field measurements (Varricchio, personal comm.).

Bentonite (Fb)

Description

This facies consists of two beds, one 1.9 m thick composed of accretionary lapilli rich in biotite, and another composed of pure ash 2.8 m thick. Both are within massive mudrock (Fm) and show especially sharp contacts below and gradational contacts above (Fig. 15).

Interpretation

This facies is interpreted to volcaniclastic ash fall deposits. Local eruptions deposited ash beds (Larsen and Nelson, 2000), later converted to bentonite (Slaughter and Earley, 1965). The bentonite beds were not radiometrically dated in this study.

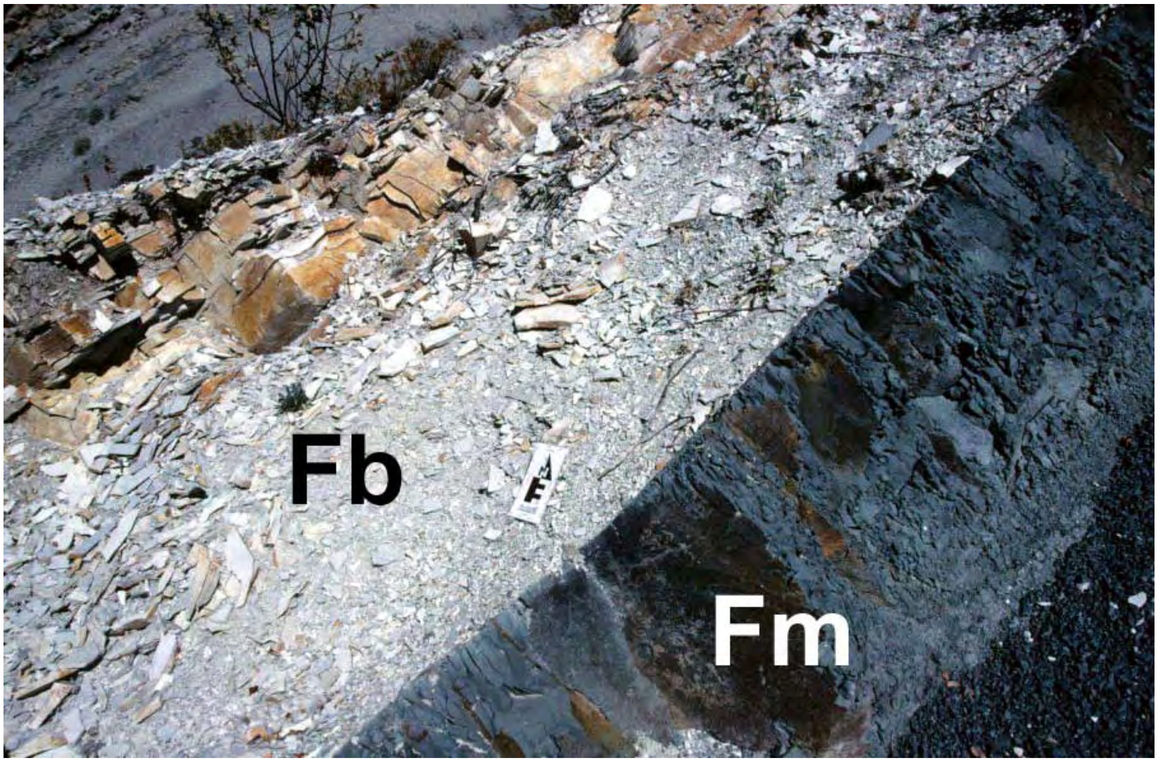

Figure 15: Contact between massive fines (Fm) and bentonite horizon (Fb). North arrow in center is 10 cm long.

CHAPTER 5

BONEBED LITHOLOGY

The Sun River Bonebed is present roughly 120 m above the base of the local stratigraphic section (Appendix B). The bonebed is a 45 cm thick conglomerate of bone and calcareous clasts in a matrix of sand and green, calcareous silty mud (Fig. 16). Examined matrix showed a uniformly very silty matrix with isolated, subrounded to rounded, very fine sand grains of 10 – 15 vol%. Rarely, the very fine sand grains reached 20 vol% in the lower 20 cm of the bed. Isolated, subrounded to subangular fine to medium sand grains were also present in all but the upper 10 cm, but never exceeding 5 vol%. No microfossils or fragments of invertebrate fossils were seen in sieved samples. Matrix color did not vary throughout the thickness of the bed.

Collected calcareous clasts were predominantly subrounded to rounded in shape, with rare occurrences of elongate and flattened (disc-like) shapes (Fig. 17). Manually broken clasts (n=12) showed internally consistent sparry calcite, with no nucleation sites. The only internal structure seen was a slight darkening of the central half in a minority of clasts (n=2), both among the largest size clasts inspected.

Fossil bone is the predominate clast type, with no more than 5 – 6 calcareous clasts encountered at any given 5 cm depth interval. Bone density (hereafter defined as the measure of bones/m^2 in a planar cross-section of the bed parallel to bedding) is high enough at the base of the bed that the conglomerate is clast-supported (Fig. 18); as bone density decreases upward, the conglomerate becomes more matrix-supported, with very

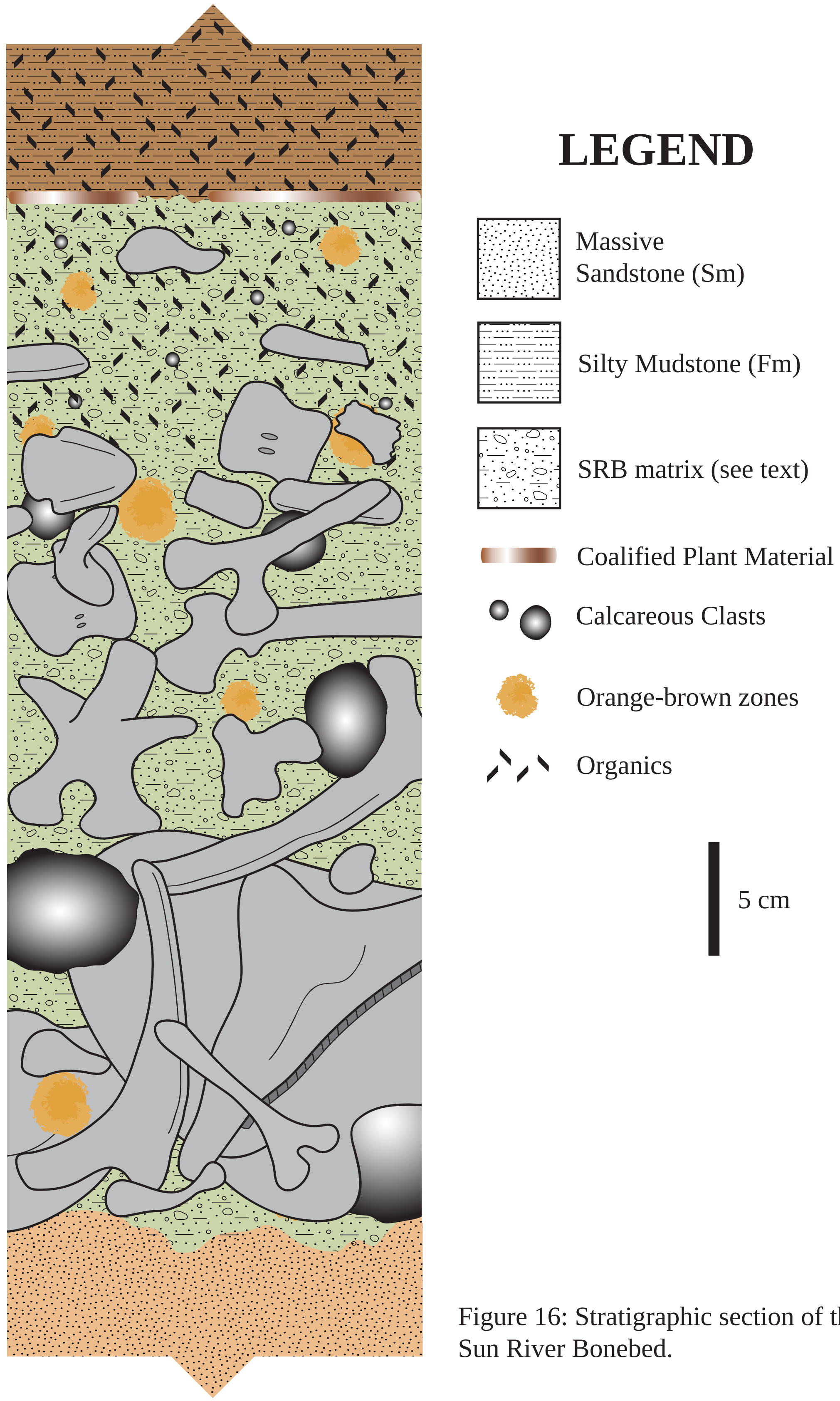

Figure 16: Stratigraphic section of the Sun River Bonebed.

Figure 17: Calcareous clasts from the SRB, with typical subrounded – rounded shape below, and rare flattened (L) and elongate (R) shapes above.

few bones and calcareous clasts in the upper 10 cm (Fig. 18). Contact between bones (clasts) is present vertically in the bed until the shallowest 10 cm (Fig. 18). Due to this vertical change in bone density, the bonebed is not lithologically specified as “matrix-supported” or “clast-supported” (Appendix B). Bones show normal grading; smaller elements (<15 cm max bone length), are ungraded, but gradually larger bones are more prevalent in respectively lower portions of the bed, with the very largest elements (50 – 60 cm max bone length) confined to the lowest 10 cm (Fig. 19). Calcaerous clasts also show an increase in diameter with depth (Fig. 18), but didn’t exhibit discrete normal grading due to their rarity. Elongate bones exhibited a preferred trend orientation, but

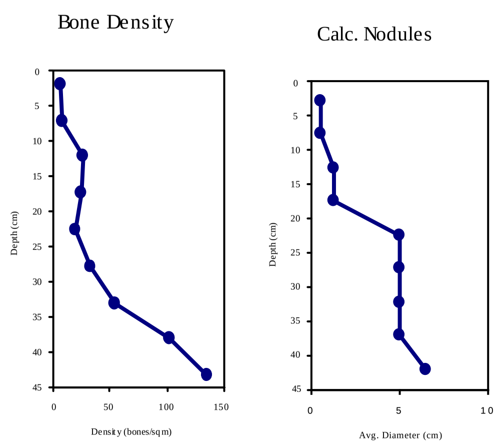

BONE DENSITY (bones/m^2)	**CALC. CLAST DIAMETER**	**TAPHONOMIC INDICATORS**	
6 bm^2	0.5 cm (diam)	Abundant plant fragments	Coalified plant material
8 bm^2			Abundant orange zones
26 bm^2	0.5 – 2 cm		
25 bm^2		Increasing density of elements, all but very largest element sizes represented	
19 bm^2	4-6 cm		
33 bm^2			
55 bm^2			
102 bm^2		Concentration of large limb bones, smaller bones persist	
135 bm^2	6-7 cm		

Figure 18: Stratigraphic description of the Sun River Bonebed, subdivided into 5 cm depth intervals. Total depth of bonebed is 45 cm. Depth increases from upper row of table downward.

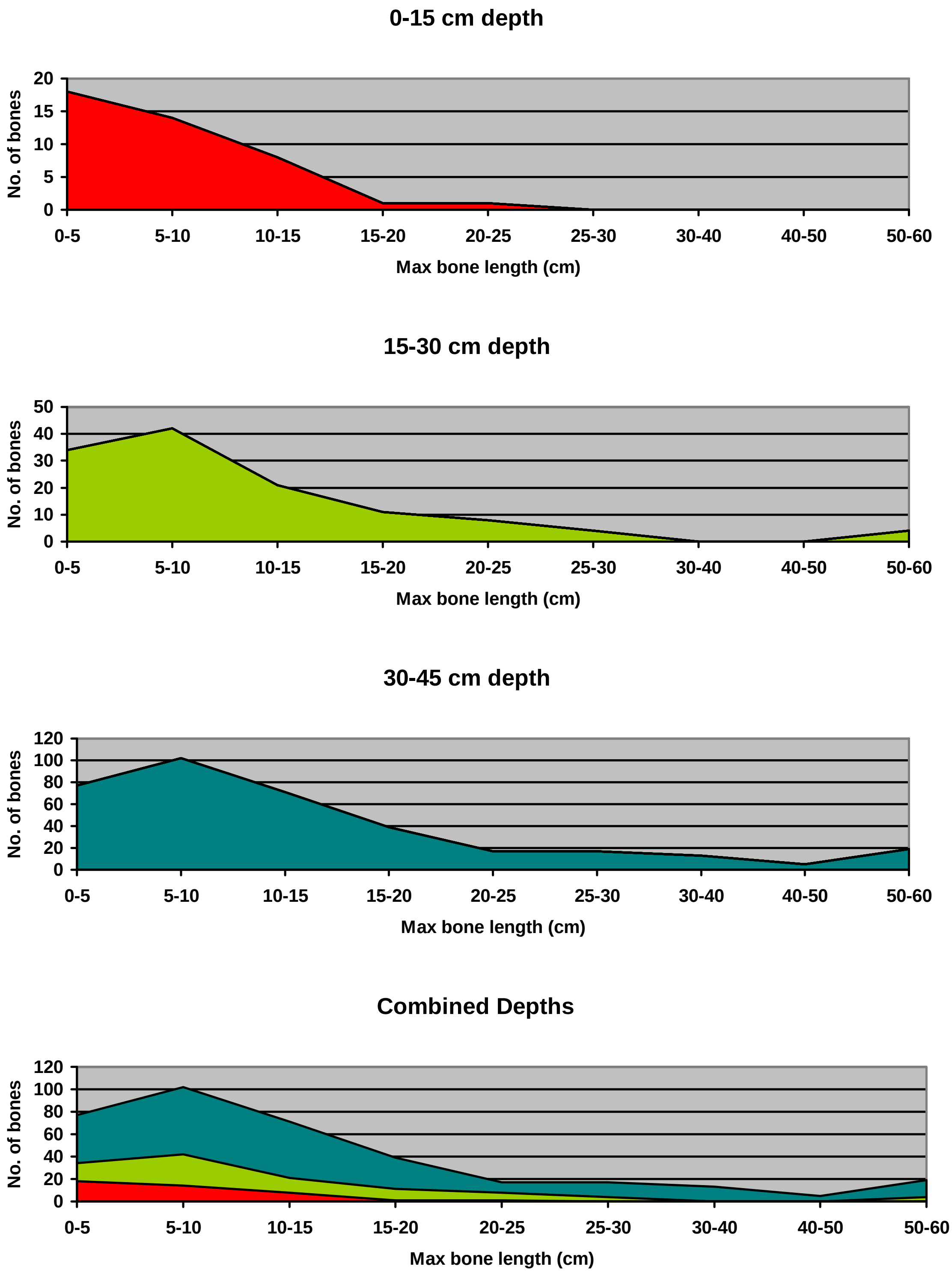

Figure 19: Population of elements, by size, over 15 cm depth intervals in the SRB. Maximum size of bones increases with depth, while population of smaller elements persists.

random plunge (orientation of bones will be discussed further in ORIENTATION OF ELEMENTS).

Organic matter, likely plant fragments, is common in the upper 10 cm of the bonebed, and large coalified plant fossils are present near the contact with the overlying massive mudrock (Fm; Fig. 20). Thin sections of the large plant fossils showed no identifiable internal structure due to the coalified condition. Occasional orange-brown zones (Fig. 21) are present throughout the bed, but are particularly common in the upper 10 – 15 cm. These zones are very friable and show no obvious shape (e.g. spherical, tubular). Bones occasionally found in these zones are especially friable and very difficult to excavate without significant damage (Figs. 21, 22). These zones are probably composed of goethite (Retallack, written comm.).

The bonebed has a sharp contact with the underlying 130 cm thick fine-grained massive sandstone (Sm; Fig. 13), with bones at the base of the bonebed occasionally protruding as much as 3 cm into the underyling bed. The underyling sandstone shows an uneven, bioturbated upper surface throughout its exposure (Fig. 23). Sieved samples of the underyling sandstone showed subrounded, moderately well sorted sand in a calcareous cement.

The bonebed has a gradational contact with the overlying 50 cm thick calcareous, brown, organic-rich, massive silty mudstone (Fm). Sieved samples from the overlying bed show a very silty mud rich in organics, and very rare, very well rounded, very fine sand grains. This overlying mudrock continues into alternating ~20 cm thick layers of red and grey.

Figure 20: Large (2.21 cm long) slab of coalified plant material near the contact between the SRB and overlying silty mudstone.

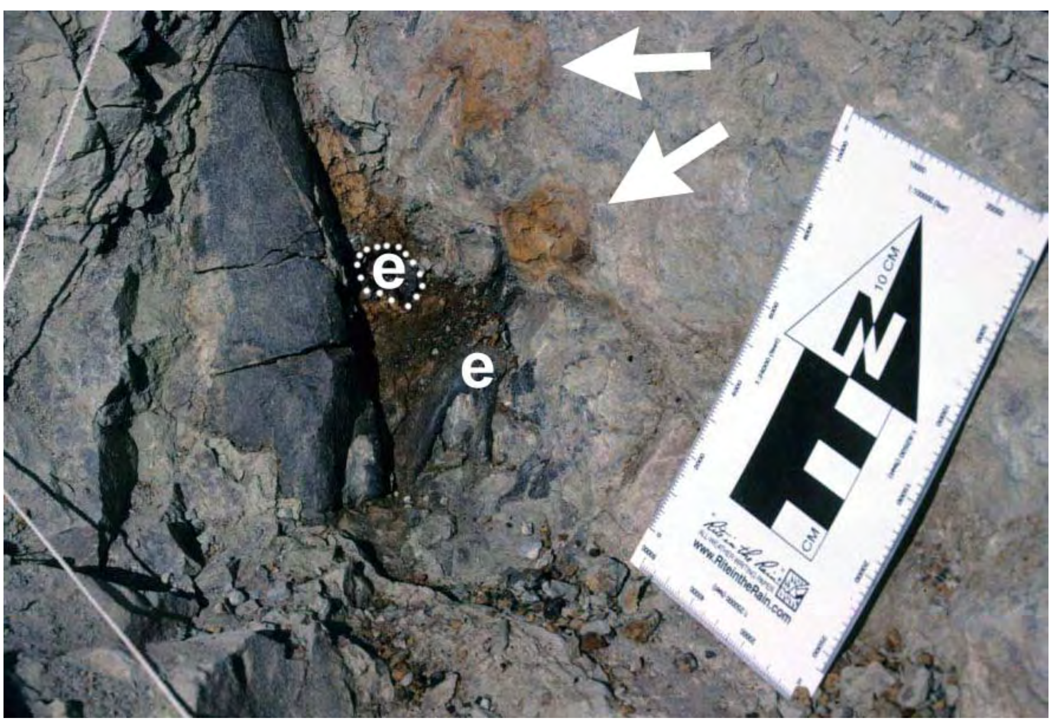

Figure 21: Orange-brown zones (arrows) near the base of the SRB. Two small elements, one outlined, are contained within a larger zone.

Figure 22: Portion of quadrate found within an orange-brown zone.

Figure 23: Exposed upper contact of massive sandstone (Sm) bed underlying the SRB, in plan view. Hammer is lying on bedding plane.

CHAPTER 6

LITHOFACIES ASSOCIATIONS

The local stratigraphy of the SRB is characterized by massive mudrocks (Fm) and various sandstone bodies (Appendix B). Massive mudrock (Fm) is the most common lithofacies; most sandstone beds are massive (Sm), and trough cross-bedded (St) and horizontally laminated (Sh) sandstones also occur. Most contacts were sharp. Gradational contacts between mudrock and sandstone bodies were present in a few beds between 75m and 85 m from the base of the section. Six distinct facies associations occurred in the SRB area strata.

Massive Mudrock

Discussion

The most common facies association in the SRB area strata is thick (commonly several m) beds of massive mudrock (Fm). Contacts with other lithofacies are sharp; contacts between massive mudrocks (Fm) and overlying sandstone bodies (commonly St) often show swaley contacts, mud rip-up clasts, trace fossils, and load casts. Both bentonite (Fb) beds were interbedded with massive fines; contacts between the massive fines and bentonite beds were sharp, with the expection of the gradational contact between the lower bentonite and the overlying massive mudrock.

Interpretation

This facies association is interpreted to represent low-energy distal overbank deposition, with vertical accretion of fines dominant (Miall, 1977). The predominance of sharp and swaley contacts and mud rip-up clasts in overlying sandstone beds, along with possible indicators of pedogenesis in massive fines (Platt and Keller, 1992; see LITHOFACIES) indicates regular subaerial exposure of the deposits. The two bentonite beds (Fb) are interpreted to represent ash fall deposits on the floodplain which are otherwise genetically independent of other sediments.

Major Tabular Sandstone

Description

The second most common facies association is thick (5.5 - 1 m), occasionally multistory tabular beds of predominantly trough cross-bedded sandstone (St), with occasional horizontally laminated sandstone (Sh), and rare massive sandstone (Sm). Contacts between multistory sandstone beds are sharp and even; upper contacts with other lithofacies are also sharp and even, while lower contacts with other lithofacies, commonly massive mudrocks (Fm), are typically swaley, and can show trace fossils or load casts, and commonly contain mid rip-up clasts or shelly lags at the base.

Interpretation

Stacked sandstone bodies can represent deposits from channels (Eberth and Miall, 1991, p. 237; Kirschbaum and McCabe, 1992; Platt and Keller, 1992), point bars (Stear, 1985), or crevasse channels and splays (Stear, 1985; Platt and Keller, 1992; Miall, 2006;

p. 171). Evidence of basal scours (swaley lower contacts, mud rip-up clasts) and lag deposits (shells) indicates these were channel deposits (Kirschbaum and McCabe, 1992; Platt and Keller, 1992; Martin and Turner, 1998). The lack of transition between different sandstone lithologies (St/Sr), absence of reactivation surfaces (Tunbridge, 1981; Eberth and Miall, 1991, p. 238), and sharp, even contacts between multistory sandstone beds indicate rapid, short-lived depositional events. The thickness of these deposits and their location in the channel is interpreted to have prevented the bioturbation and bedding destruction that affected thinner sandstones (discussed in following lithofacies association). The sandstone containing the MOR 1130 specimen below the SRB (see Appendix B), while massively bedded, was likely not subject to bioturbation, considering the thickness of the bed (3.5 m). This bed might have been a result of rapid deposit from bank collapse and liquefication, given the even vertical distribution of gastropod fossils and plant material in the bed (Varricchio, personal comm.).

Minor Tabular Sandstone

Description

Thinner (0.3 - 1 m) tabular sandstones also occur, but are not multistory except for two beds ~6.6 m from the base. Beds are exclusively massive, and contacts with other lithofacies are sharp. The minor tabular sandstone underlying the SRB (*SRB* on Appendix B) shows an uneven, bioturbated upper contact, while another minor tabular sandstone shows load casts on its lower contact with massive mudrock.

Interpretation

The minor tabular sandstones are interpreted to represent high-energy crevasse channel and proximal crevasse splay deposits (Stear, 1985; Platt and Keller, 1992; Miall, 2006; p. 171). The bioturbated upper surface of one bed is common to crevasse deposits (Platt and Keller, 1992); the predominance of massively bedded sandstone is interpreted, in part, to be a result of the associated bioturbation. Most beds do not show similar surfaces; the bioturbated surfaces could have been lost to erosion, or these beds could have been the result of rapid deposition, without being subject to bioturbation (Lowe, 1982; G. A. Smith, 1986).

Alternating Mudrock and Sandstone

Description

Lesser occurrences of thin (<0.3 m) interbedded massive mudrock (Fm) and horizontally laminated sandstone (Sh) or massive sandstone (Sm) are found 67 m, 96.5 m, 114 m, 138.5 m, 147 m, and 155 m from the base of the section. Mudcrack casts, molds from eroded mud rip-up clasts, and unidentified trace fossils are found at the base of sandstones in this association. Interpreted trace fossils of the *Coprinisphaera* ichnofacies are found in massive sandstones (Sm) in this facies association. Contacts between mudrocks and sandstones are sharp. Contacts with other lithofacies are commonly sharp and even, with rare occurrences of swaley upper contacts with trough cross-bedded sandstone (St) and thicker massive sandstone (Sm).

Interpretation

This facies association is interpreted to represent low-energy deposition with fluctuating water levels (Jackson, 1978; Eberth, 1993). Interbedded sandstones and fines can represent levee deposits (Smith and Smith, 1980; D. G. Smith, 1986; Platt and Keller, 1992), but these deposits typically show root traces (Smith and Smith, 1980) and thicker fines relative to sandstones (Platt and Keller, 1992), and the sandstones are commonly dominated by ripple-cross laminated sandstones (Sr) as a result of their proximity to the main channel (Nadon, 1994).

The even thickness of the sandstones and fines (Mossop and Flach, 1983), and the dominance by massive (Sm) and medium to coarse-grained horizontally laminated (Sh) sandstones, suggests these deposits were instead low-energy distal crevasse splay deposits (Nadon, 1994). These deposits resulted from a combination of vertical accretion of fines (Miall, 1977), and deposition of sand, with flow distal enough from the main channel to deposit only low-energy (Sm/Sh) sand bodies. Mudcrack casts, mud rip-up clasts, and trace fossils suggest regular subaerial exposure and bioturbation of the beds; in fact, the crevasse splay deposits of Nadon (1994, p. 458) also show “monospecific, open burrows probably formed by insects.”

Gradational Sandstone and Mudrock

Description

Rare occurrences of massive mudrocks (Fm) and massive sandstone (Sm) with gradational contacts are between 100 m and 115 m from the base of the section. The beds predominantly fine upward (Sm → Fm), with one occurrence of coarsening upward (Fm → Sm). Contacts between successive sequences or with other lithofacies are sharp and even.

Interpretation

This facies association is interpreted to represent individual depositional events with a rapid shift in energy. While the fining-upward sequences can result from the filling of abandoned channels (Miall, 2006, p. 177-178), the lack of indicators of standing water (laminated fines, freshwater fossils) suggests deposition from individual distal overbank flooding episodes (Kirschbaum and McCabe, 1992). A coarsening-upward sequence can result from a subaqueous delta deposit (Tye and Coleman, 1989; Kirschbaum and McCabe, 1992) but this is unlikely, for the same lack of indicators of standing water listed above. Instead, this association likely represents the distal progradation of a crevasse splay (Kirschbaum and McCabe, 1992).

Gradational Conglomerate and Sandstone

Description

At the top of the section, there is one occurrence of fining upward from matrix-supported massive conglomerate (Gmm) → trough cross-bedded sandstone (St) → ripple cross-laminated sandstone (Sr). Contacts with overlying and underlying beds, as well as the contact between the trough cross-bedded sandstone (St) and ripple cross-laminated sandstone (Sr) are obscured. The contact between the matrix-supported massive conglomerate (Gmm) and trough cross-bedded sandstone (St) is sharp and swaley, with mud rip-up clasts at the base of the sandstone.

Interpretation

This facies association could represent deposition by a meandering channel or by a high-energy flood. The association resembles the lag deposit → St → Sr progression of a “classic” lateral accretion deposit (Brierley, 1996), but it is difficult to attribute this association to a meandering system without any vertical or lateral repetition of the sequence. It is also possible that this deposit is the result of an individual flood surge, which could have been deposited on the floodplain (Stear, 1985), or proximal to the main channel (Kirschbaum and McCabe, 1992).

Summary

Interpretation of Depositional Environment

Many of the features of the interpreted channel deposits are common to ephemeral stream deposits, including: tabular, thick, clean crossbedded sandstones with abundant rip-up clasts (Lorenz, 1981; Eberth et al., 2006), uniform thickness of beds for more than 100 m (Lorenz, 1981; Tunbridge, 1981), erosive basal surfaces with relatively little relief (<15 cm), absence of lateral accretion deposits or merged channel deposits, absence of reactivation surfaces (Tunbridge, 1981), and convolute laminae in horizontally laminated sandstone (McKee et al., 1967). The channel sandstones of the SRB strata are interpreted to be deposits of an ephemeral stream.

The remaining beds in the SRB area are interpreted to represent associated ephemeral overbank deposits. Crevasse channel and proximal crevasse splay deposits are represented by minor tabular sandstones; while distal crevasse splay deposits are represented by alternating sandstone and mudrock, and the gradational coarsening-upward mudrock and sandstone. Flooding events on the floodplain are represented by the massive mudrocks and gradational fining-upward sandstone and mudrock. The gradational conglomerate and sandstone at the top of the section could represent channel deposits, or proximal overbank deposits from a flood. If this fining upward sequence represents a channel deposit, it remains unclear why this channel deposit is sedimentologically different from the lower tabular, structurally uniform channel deposits. Deposition of the bonebed will be discussed later in DISCUSSION.

It does not appear that sediments were exposed to exclusively wet or dry conditions in periods of exposure. Red-colored mudrocks signify subaerial, semi-arid to arid exposure (Miall, 2006, p. 421), while abundant trace fossils, preservation of plant material, grey to green colored mudrocks (Eberth and Miall, 1991), and load casts indicate waterlogged or moist substrate. Additionally, trace fossils from the *Coprinisphaera* ichnofacies, present in thin interbedded sandstone and mudrock approximately 2.3 m below the SRB, have been interpreted as insect burrows associated with exposed sediments subject to pedogenesis under warm, humid conditions (Genise et al., 2000; Alonso-Zarza and Silva, 2002; Melchor et al., 2002).

Comparison to Previous Interpretations

Tabular channel deposits in the upper Two Medicine are unusual - channel sandstone bodies in the middle and upper Two Medicine are characteristically lenticular and show low width/depth ratios, interfingering with finer beds, and rapid lateral thinning into extensive "wings" (Lorenz, 1981; Lorenz and Gavin, 1984; Rogers, 1995); while tabular channel sandstones are commonly found in the lower Two Medicine instead (Lorenz, 1981; Lorenz and Gavin, 1984; Roberts, 1999).

Ephemeral stream deposits, however, are more common in the upper Two Medicine. In fact, some channel sandstones in the upper Two Medicine, while showing low width/depth ratios, are interpreted to represent ephemeral stream deposits (Shelton, 2007). In addition, sandstones similar to the minor tabular sandstones of the SRB strata, with tabular shape, massive bedding, and bioturbated upper contacts, have been interpreted as overbank deposits in the middle and upper Two Medicine (Lorenz, 1981; Lorenz and Gavin, 1984). In particular, many of the overbank sandstone bodies in the upper Two Medicine have been interpreted as the deposits of seasonal, widespread, high-energy depositional events (Lorenz, 1981; Lorenz and Gavin, 1984), like the associated ephemeral floods interpreted to be responsible for many of the SRB area overbank deposits. Lorenz (1981, p. 138) even states such "episodic, high magnitude depositional events" were "the norm" in the upper Two Medicine.

CHAPTER 7

TAPHONOMIC DATA

Taxonomic Composition of SRB

The SRB bone assemblage consists of 568 catalogued elements, of which 9.7% (n=55) are unidentifiable. Unidentifiable fragments are included in weathering, abrasion, and fracture counts only. Of the identifiable elements, 98% (n=505) are assignable to Hadrosauridae (Table 2). Among elements which diagnose between Hardosauridae and Lambeosaurinae, all such diagnostic elements (n=76) could be further assigned to Lambeosaurinae (e.g. see Figs. 24, 37). Identifiable synapomorphies of Lambeosaurinae include: height/width ratios >3.5:1 of dorsal neural spines, a deltopectoral crest greater than 50% of the width of the humerus, a scapular neck narrower than the blade, and flaring of the ischial boot (Horner et al., 2004). The minimum number of individuals (MNI) is 8, based on the number of left dentaries collected. All complete femurs (n=6) are similar in length (53-60 cm), with a size diagnosed as late juvenile by Horner et al. (2000). All other identifiable elements are consistent with late juvenile size (Table 3), with the exception of an individual humerus intermediate in size to the *Hypacrosaurus* nestling and juvenile age classes described by Horner and Currie (1994) (Horner, personal comm.; Fig. 24).

The remaining 1.6% of elements (n=8) includes an unknown theropod bone, turtle shell fragments, a possible lizard/amphibian bone, a tyrannosaurid tooth fragment, and a previously collected *Unio* shell (Table 4), the latter two of which were likely float. Due to

Table 2: Hadrosaurid elements recovered from the Sun River Bonebed. * = assignable to Lambeosaurinae.

	ELEMENT		COUNT
Cranial	Atlas		2
	Basioccipital		1
	Dentary		12
	Exocippital		3
	Frontal		4
	Jugal		1
	Maxilla		5
	Nasal*		1
	Occipital Condyle		1
	Postorbital		2
	Prefrontal		2
	Premaxilla*		4
	Quadrate		6
	Squamosal		1
	Supraoccipital		2
	Unknown skull		6
Axial	Centrum:	Cervical	2
		Dorsal	12
		Sacral	2
		Caudal	17
		unknown	12
	Chevron		23
	Neural Arch (inc frag):	Cervical	27
		Dorsal*	43
		Sacral	2
		Caudal	57
	Rib (inc frag):	Cervical	4
		Dorsal	126
		Sacral	2
	Transverse Process	Sacral	2
		Caudal	2
Pectoral Girdle	Humerus*		11
	Metacarpal		8
	Phalange		1
	Radius		9
	Scapula*		8
	Sternum		5
	Ulna		7
Pelvic Girdle	Astragalus		1
	Femur		10
	Fibula		11
	Ilium		8
	Ischium*		9
	Metatarsal		9
	Phalange		7
	Pubis		10
	Tibia		5
		TOTAL	505

Table 3: Mean length of limb bones common to the SRB.

ELEMENT	**n** (**COMPLETE ELEMENTS**)	**MEAN LENGTH**
Femur	6	57.3 cm
Fibula	1	50.5 cm
Humerus	1*	27 cm
Metacarpal III	4	14.8 cm
Metatarsal III	4	23 cm
Radius	3	35.3 cm
Tibia	4	54.3 cm
Ulna	4	37.4 cm

* *element count does not include unusually small humerus*

Figure 24: Unusually small humerus inconsistent with typical humeri size (above) of the SRB elements.

Table 4: Taxa recovered from the Sun River Bonebed.

TAXA	**MNI**	**NISP**
Lambeosaur indet	8	515
Tyrannosaur indet	1	1
Unknown Theropod	1	1
Turtle	1	4
Lizard / Amphibian	1	1
Unio sp.	1	1

only minor screening, microvertebrate material was not considered. Macrovertebrate (>1 cm^3) elements are likely very well represented, considering the extremely high density of bones, distinct color difference between bone and matrix, and the careful collection procedures followed.

Orientation of Elements

Trend and plunge were measured for elongate (2:1 or greater) bones during the 2004 excavation. Orientations were palinspastically restored, and the resulting rose diagram plotted for these elements (n=212) was transformed into a mirror-image rose diagram (Fig. 25) and analyzed for preferred orientation of strike using the methods of Shipman (1981, p. 69-76). Using these methods, the minimum range needed to include at least 50% of measured elements would be the 50° range from 340° to 10° (red, Fig. 25). This is interpreted to show a preferred orientation, as this range would account for less than 30% of measured elements in a randomly oriented set.

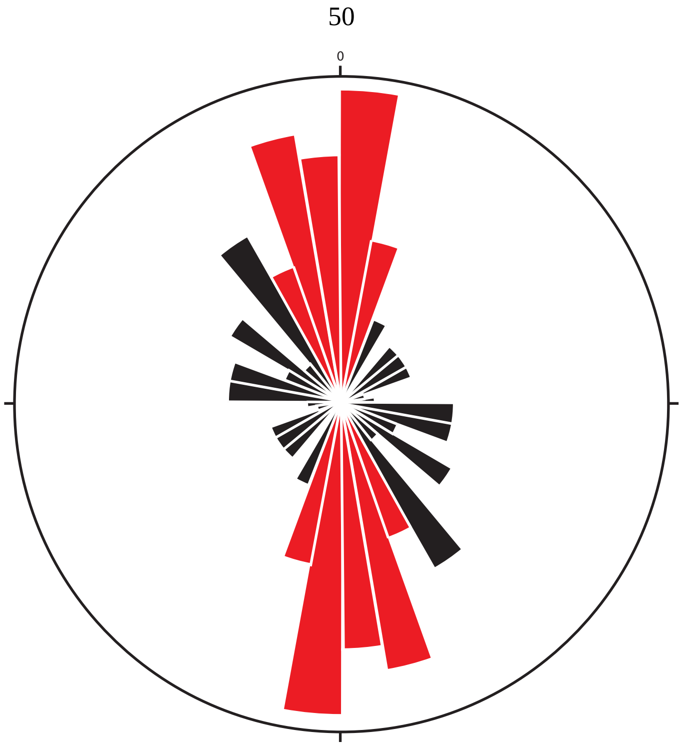

Figure 25: Mirror diagram of trend of long axes for measured elements in the SRB. r = 14.

Plunges of mapped elements were also analyzed for evidence of preferred orientation in three dimensions using the methods of Fiorillo (1988a). This plot (Fig. 26) showed a random distribution of elements in three dimensions (Fiorillo, 1988a).

During excavation, large limb bones such as femurs and tibia were occasionally bound parallel by smaller elongate elements, sometimes on opposing sides of the larger element (Fig. 27). However, parallel alignment of the smaller elements was not significantly higher near large bones than in the assemblage as a whole.

Elements within the SRB are almost exclusively disarticulated, with only two instances of articulation – a pair of articulated exocippitals and an articulated frontal and prefrontal. Due to the extremely high bone density within the bed (exceeding 100 bones/m^2), the relatively small area which was excavated (approximately 1.5 m^3), and the

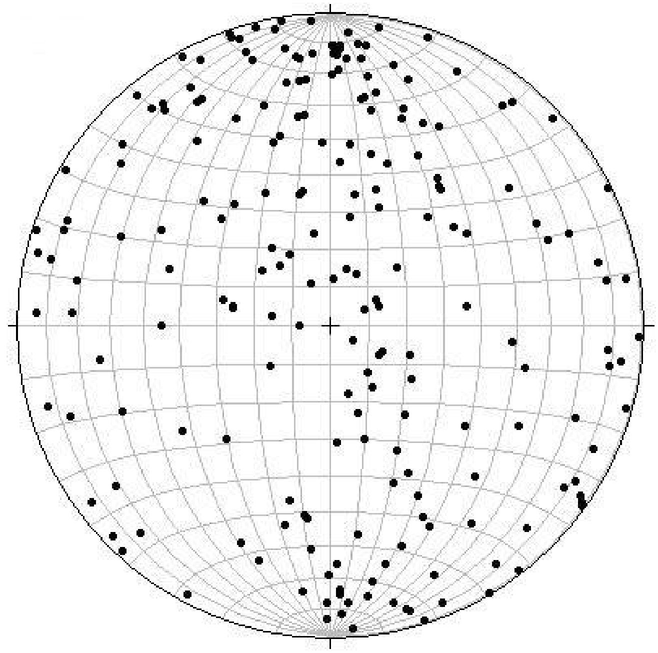

Figure 26: Scatter plot of plunge of long axes of measured elements in the SRB.

Figure 27: Smaller elongate elements (I,II,IV) parallel and adjacent to a larger tibia (III). Central tibia also in contact with two other non-elongate elements below (V,VI). View parallel to bedding plane, in lower right corner of rightmost grid.

consistency in size, color, and modification of elements (Appendix A), evidence of association was difficult to detect. But, review of the bonebed map (Appendix A) after element identification did not show any signs of apparent association.

Spatial Distribution of Elements

As discussed in BONEBED LITHOLOGY, elements are unevenly distributed vertically within the bed. In the basal 10 cm of the bonebed, bone density is exceptionally high (100-130 bones/m^2; Fig. 18), and it is not uncommon for an element to be in contact with as many as five or six others (Fig. 27). Bone density gradually decreases upward, and remains near ~25 bones/m^2 in the middle 15 cm of the bed (Fig. 18). Bone density in the upper 10 cm of the bed was very low (<10 bones/m^2; Fig. 18).

The largest limb bones (femur, tibia) are restricted to the densest lower 20 cm of the bed. Bones of intermediate size are evenly distributed in the lower 30 cm of the bed, and small elements are present throughout the entire bed. Sorting among smaller elements in the shallow depths of the bed was not detected, with equal abundance of compact, spongy bones (unguals, vertebrae) and denser cranial bones.

Element Representation

Considerable variation exists among the frequency of elements in the SRB. Individual elements were grouped into categories based on bone structure, density, and size, to allow for testing of element distribution using a χ^2 test for equality of distributions. The groups of elements were tested against an ideal accumulation with the same NISP as the SRB bonebed, but with elements present in identical percentage to that of a typical lambeosaur skeleton (Table 5; sensu Varricchio, 1995). The χ^2 test indicated the SRB accumulation is significantly different ($p<0.001$) from that of an ideal accumulation, with certain groups of elements contributing to this variation more than others (Table 5).

Overrepresented elements include limb bones (humeri, femora, tibii, etc), pelvic elements (ilia, ischia, pubes), ribs, and heavier cranial elements (dentaries and maxillae) (Fig. 28; Table 5). With the exception of ribs, these elements are representative of Voorhies Group III elements (Voorhies, 1969; Lehman, 1982): dense, robust bones commonly left behind as fluvial lag deposits. Underrepresented elements include vertebral processes (neural arches, chevrons, transverse processes), sacral elements, phalanges, carpals, tarsals, and light cranial elements (all other cranial bones besides dentaries and maxillae) (Fig. 28; Table 5). These elements are similar to the easily transportable elements of Voorhies Group I (Voorhies, 1969; Lehman, 1982). Elements with no significant difference of representation, pectoral elements (scapulae, sterna, coracoids), vertebrae, and metapodials, display a variety of form and structure, representing elements from all Voorhies Groups (Voorhies, 1969).

The respective overrepresentation and underrepresentation of certain elements indicates selective removal of smaller elements, which could occur through more than one process. The possibility of removal of smaller elements through scavenging is unlikely, as significant scavenging of the carcasses would have left abundant tooth marks and shed carnivore teeth, which are almost nonexistent in the SRB accumulation (n=4 for

Table 5: Comparison of expected and observed (SRB) counts of individual elements. Abundances (+, overrepresented; -, underrepresented) are for SRB counts relative to expected counts. Values for expected counts based on Horner et al. (2004).

Element	Expected Count	Observed Count	$(O-E)^2/E$	Abundance
Humerus	2.5	11		
Fibula	2.5	11		
Femur	2.5	10		
Radius	2.5	9		
Ulna	2.5	7		
Tibia	2.5	5		
Limb Bones	**15**	**53**	**96.27**	+
Scapula	2.5	8		
Sternum	2.5	5		
Coracoid	2.5	0		
Pectoral Elements	**7.5**	**13**	**4.03**	no change
Pubis	2.5	10		
Ilium	2.5	8		
Ischium	2.5	9		
Pelvic Elements	**7.5**	**27**	**50.70**	+
Dorsal NA	22.5	43		
Caudal NA	73.75	57		
Cervical NA	16.26	28		
Atlas	2.5	2		
Chevron	69.375	23		
Caudal TP	18.75	2		
Vertebral Processes	**203.125**	**154**	**11.88**	-
Caudal Vert	75	17		
Dorsal Vert	22.5	12		
Cervical Vert	17.5	2		
Axis	1.26	0		
Vertebrae	**41.25**	**31**	**2.55**	no change
Dorsal Ribs	22.5	126		
Cervical Ribs	16.26	4		
Ribs	**38.75**	**130**	**214.88**	+
Sacral Vert	13.125	2		
Sacral Ribs	13.125	2		
Sacral TP	13.125	2		
Sacral NA	13.125	2		
Sacral Elements	**52.5**	**8**	**38.72**	-

Table 5: continued

Carpus	1.875	0		
Manus Digits	15	1		
Calcaneum	2.5	0		
Pes Digits	15	7		
Astragalus	1.26	1		
Digital Elements	**36.625**	**9**	**19.89**	-
Metacarpals	5	8		
Metatarsals	3.75	9		
Metapodials	**8.75**	**17**	**7.78**	no change
Lacrimal	2.5	0		
Quadratojugal	2.5	0		
Parietal	2.5	0		
Parasphenoid	1.26	0		
Laterosphenoid	1.26	0		
Orbitosphenoid	1.26	0		
Presphenoid	1.26	0		
Basipterygoid	1.26	0		
Basisphenoid	1.26	0		
Prootic	1.26	0		
Opithospenoid	1.26	0		
Vomer	1.26	0		
Palatine	1.26	0		
Pterygoid	2.5	0		
Ecopterygoid	2.5	0		
Predentary	1.26	0		
Surangular	2.5	0		
Articular	2.5	0		
Prearticular	2.5	0		
Sclerotic Ring	2.5	0		
Stapes	2.5	0		
Ceratobranchial	1.26	0		
Palpabrel	2.5	0		
Nasal	2.5	1		
Jugal	2.5	1		
Squamosal	2.5	1		
Frontal	2.5	4		
Supraoccipital	1.26	2		
Exocippital	2.5	3		
Prefrontal	2.5	2		
Postorbital	2.5	2		
Basioccipital	1.26	1		
Condyle	1.26	1		
Premaxilla	1.26	4		
Quadrate	2.5	6		

Table 5: continued

Light Cranial Elements	**67.5**	**29**	**23.11**	-
Maxilla	2.5	5		
Dentary	2.5	12		
Heavy Cranial Elements	**5**	**17**	**21.80**	+
			$\chi^2 \approx$ **497**	**p <0.001**

tooth marks, Table 6). In addition, carnivore activity is focused on the parts of a carcass with the most meat and viscera, the limbs, abdominal area, and rib cage (Blumenschine, 1986). Carnivore “winnowing” would have removed the elements associated with these parts of the body, but in the SRB, limb bones, pelvic elements, and ribs are instead overrepresented (Fig. 28). The possibility of removal of smaller elements through weathering is also unlikely, as there was no higher degree of weathering of smaller elements versus larger (weathering discussed further below). It is more likely the SRB assemblage experienced hydraulic winnowing, with the selective removal of lighter, more easily transportable elements.

Weathering and Abrasion

Weathering was assessed for all elements displaying sufficient surface exposure (not obscured by calcite covering or adhered matrix) and for fragments not resulting from collection fracture (fractures induced during excavation). Behrensmeyer (1978) established six weathering stages (0-5) in modern assemblages, based on physical modification to the surface of bones. Fiorillo (1988b) later modified these into the four (0-3) stages used in this study: stage 0 shows no signs of surface cracking or flaking,

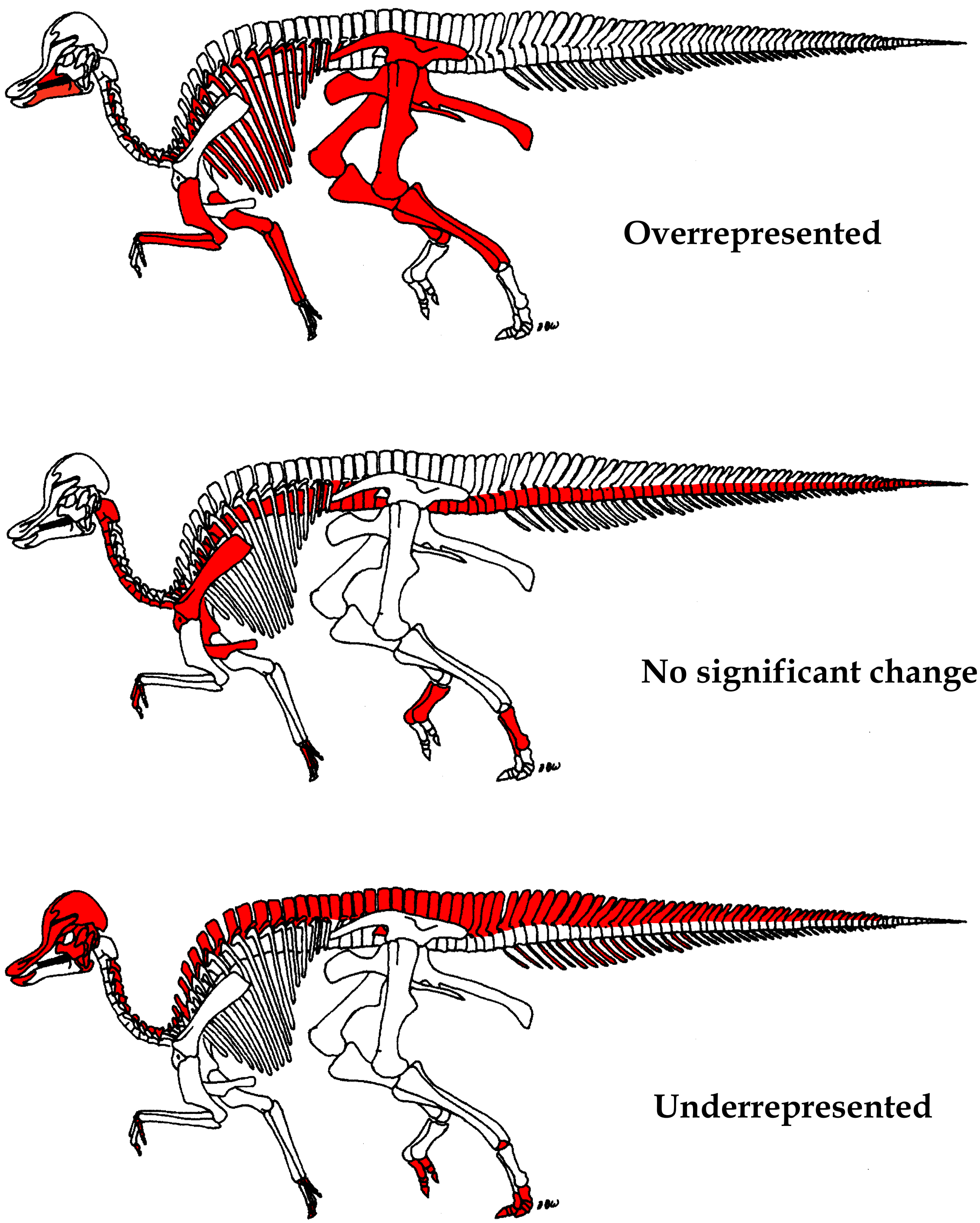

Figure 28: Representation of elements in the SRB compared to an ideal accumulation, after Davis et al. (2000). Figure from Horner et al. (2004).

Table 6: Bone modification of elements recovered from the Sun River Bonebed.

FEATURE		COUNT	PERCENTAGE
WEATHERING STAGE			
	0	452	97.6
	1	11	0.4
	2	0	0.0
	3	0	0.0
		n = 463	
ABRASION			
	0	204	63.1
	1	112	34.7
	2	7	2.2
		n = 323	
FRACTURING			
	Spiral	63	43.2
	Transverse	61	41.8
	Other	22	15.0
		n = 146	
OTHER			
	Fragments	55	
	Tooth Marks	4	
	"Wet Rot"	59	

stage 1 shows cracking parallel to bone fiber, stage 2 shows flaking in addition to parallel cracking, and stage 3 shows loss of the outermost bone layer and exposure of internal fibrous bone. Weathering of SRB elements is minimal., with over 97% (n=452) of 463 analyzed elements showing weathering stage 0 (Fig. 29; Table 6). The remaining elements were exclusively weathering stage 1 (n=11; Fig. 29), with no occurrences of stages 2 or 3. No elements showed evidence of differential weathering. The weathering stages of excavated elements suggest subaerial exposure was minimal; Behrensmeyer (1978) suggested the presence of only stages 0 and 1 indicates a maximum of two years exposure.

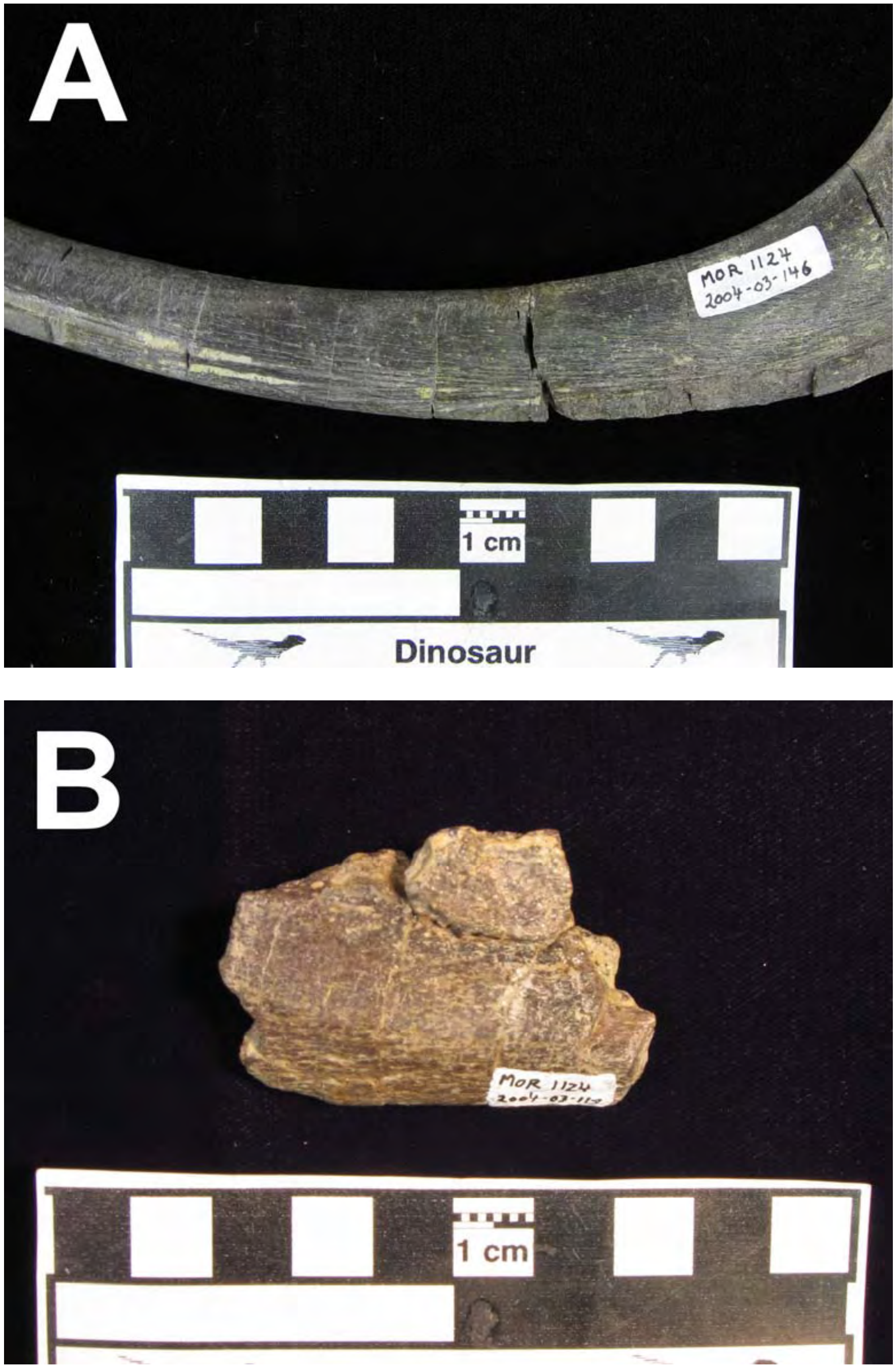

Figure 29: Characteristic weathering stages seen in the SRB elements. Stage 0 (A) on a dorsal rib and stage 1 (B) on an unknown fragment.

Elements not displaying extensive collection fractures were also inspected for abrasion. Of the 323 elements analyzed, over 63% (n=204) showed little to no abrasion (stage 0) (Fig. 30; Table 6). Of the remaining elements, most showed moderate abrasion (34.7%, stage 1; Fig. 30), with rare occurrences (2.2%) of heavy abrasion (stage 2; Fig. 30). The majority of elements in SRB were unabraded, however, lack of abrasion does not necessarily imply a lack of transport, as fresh bone can experience significant (100's of hrs) transport without abrasion (Fernandez-Jalvo, 1988). The percentage of moderately abraded elements (stage 2) and rarity of heavily abraded (stage 3) elements suggests that while transport of elements occurred, it was not extensive. Abraded elements commonly showed equal abrasion to all edges, suggesting transport occurred after disarticulation. Abrasion was also equally divided among fractured and complete elements, with abrasion common along fractured edges (fractures discussed further below).

Elements showing moderate weathering (stage 1) were evenly divided among complete, partial., and fragmentary elements, and the majority (66%) of elements showing heavy abrasion (stage 2) were complete elements. Ryan et al. (2001) considered heavily abraded, highly weathered, fragmented elements in a predominantly unweathered and unabraded assemblage to represent a subset of allochtonous or reworked “background” material independent of the rest of the accumulation. The dearth of such elements in the SRB suggests there was very little “background” material within the assemblage, indicating a common taphonomic history for the majority of the bonebed.

Figure 30: Characteristic abrasion stages in the SRB elements. Unabraded (stage 0) prefrontal (A), moderately abraded (stage 1) rib shaft (B), and heavily abraded (stage 3) fragment.

Bone Breakage and Fracturing

In his work on modern large mammal assemblages, Haynes (1983a) established three major fracturing surfaces on long bones: transverse, spiral, and longitudinal. For SRB elements, fractures with an outline of a helix or partial helix (Fig. 31), or showing evidence of peeling of cortex, were interpreted as spiral. Smoother fractures perpendicular to the long axis were interpreted as transverse (Fig. 31). Occasionally, fractures on non-long bones were considered spiral or transverse where appropriate. Additional styles of fracturing were observed, some similar to percussion marks in archaeological literature (see Lyman, 1994, p. 275-276; Fig. 31), and some resembling gouged or scalloped depressions in bones (Fig. 32). However, due to the rare occurrence of these types of fracture, and their indistinct taphonomic significance, these were grouped with indeterminant fractures (fractures which cannot be reliably placed in one category) as "other." Collection and longitudinal fracture, two fracture styles common to taphonomic studies, were not counted here; collection fracture due to its minimal taphonomic significance, and longitudinal because it was difficult to discern pre-fossilization crushing from the results of lithostatic compaction, which was particularly common, as evidenced by numerous warped elements.

Overall, the SRB elements are unfractured, with only 23% of all elements showing signs of fracturing (n=131 elements, representing 146 fractures). The most common types of fracturing are spiral and transverse, accounting for 43% (n=63) and 42% (n=61) of fractures, respectively (Table 6). Though the significance of these types of fractures is controversial, their abundance suggests the bones were relatively fresh

Figure 31: Common fracture types seen in the SRB elements. Spiral fracture of dorsal rib capitulum (lower) and rib shaft (upper) (A), transverse fracture on both ends of an ilium (B).

Figure 32: Uncommon fracture types seen in the SRB elements. Fracture similar to percussion mark on a humerus shaft (A), "gouged" fracture on a radial epiphysis (B).

when broken (Haynes, 1983a; Morlan, 1980), This agrees with some of the observed "indeterminant" fractures, particularly the "chipping" or "flaking" of edges of flat, thin bones such as the blades of ishchia and pubes (Fig. 33). Such fractures are similar to observed trampling fractures of relatively fresh large mammal scapula (Gifford, 1984). Rarely, elements appeared to be fractured in situ, with fractured portions of the respective elements showing opposing sides of fractures separated by less than 1 cm (Fig. 34). Other fractured portions of elements, separated by up to 15 cm, were found to fit together after lab preparation (Fig. 35).

Figure 33: Fracturing on the edge of pubis blade, a fracture style commonly seen on flat, thin bones in the SRB.

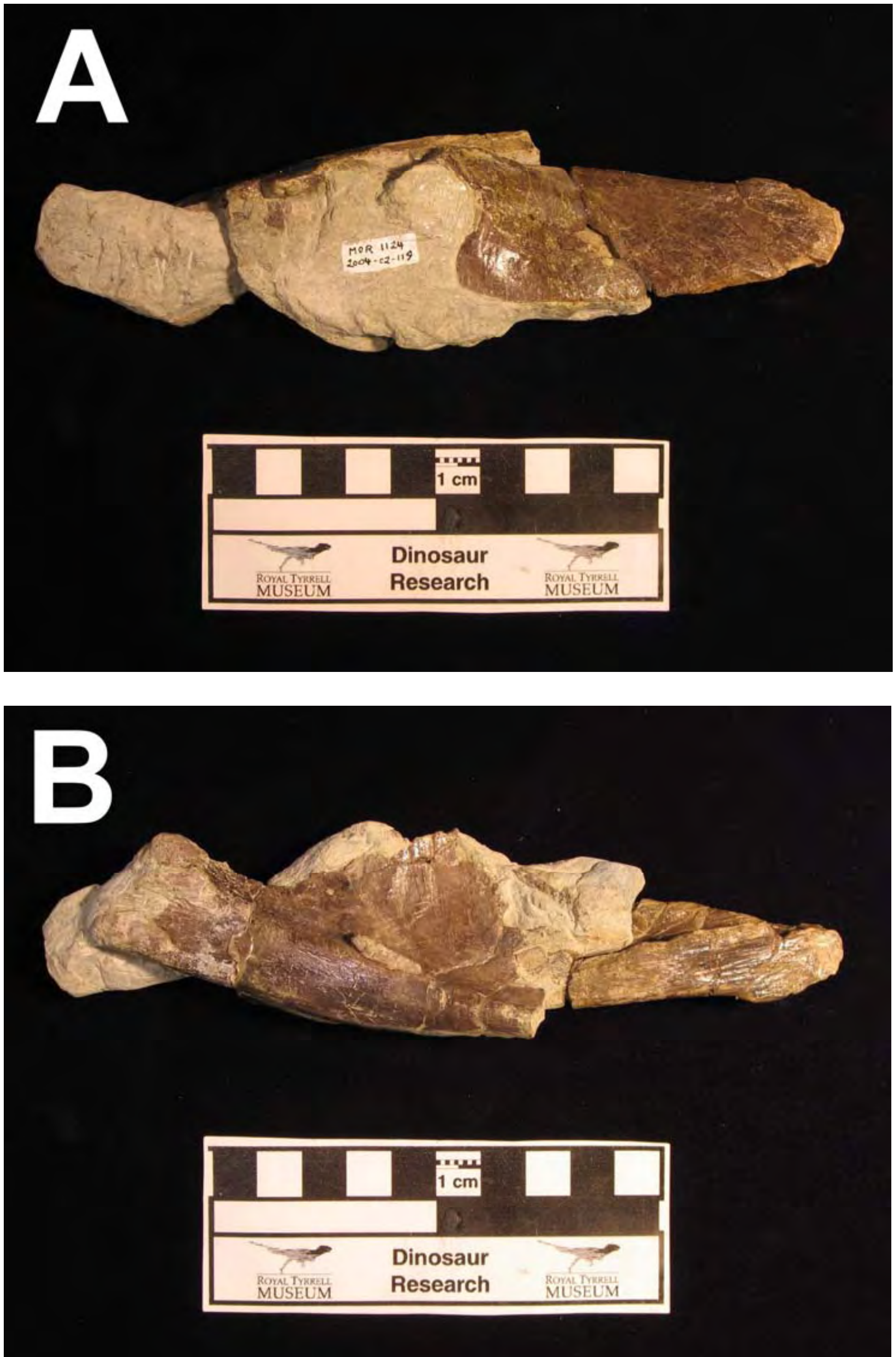

Figure 34: Right quadrate showing a transverse fracture along the longitudinal midline, in lateral (A) and medial (B) view. Fractured portions preserved in near original position in element.

Figure 35: Two pieces of preacetabular process of left ilium. Specimens fit well after preparation, but were separated by 15 cm in situ.

<u>“Wet Rot”</u>

A unique form of bone modification, termed “wet rot,” was observed on a number of elements from the SRB. The epiphyses of almost all long bones are distinguished by what appears to be corrosion of the cortex, a condition reminiscent of weathering state 3 (Fig. 36; Fiorillo, 1988b). This epiphyseal corrosion was predominantly observed on long bones, but was also observed on the ends of processes on ischial shafts, pubes, neural arches, and centra (Fig. 37).

This corrosion is unlikely to be the result of weathering, as it exists on both epiphyses of long bones with almost no weathering along the shaft (Fig. 36). It is unlikely to be a form of abrasion, as it is also seen on unabraded epiphyses (Fig. 38). Pressure

Figure 36: Infered “wet rot” of epiphyses common to long bones in the SRB. Note pitted, weathered appearance to epiphysis, in contrast to the unweathered shaft.

Figure 37: Interpreted “wet rot” seen on an ishchial boot (A) and caudal centrum (B).

Figure 38: Interpreted "wet rot" on a metatarsal III epiphysis. Note unabraded articular surface of epiphysis.

solution between bones is also unlikely, as this corrosion is found around the circumference of epihyses and occurs on elements not in contact with other bones. Haynes (1983a) desribes cortical bone flaking off modern mammal bones, but this is mainly along shafts, and a result of carnivore gnawing. Neotaphonomic studies on modern bone suggest a more likely process. In several studies of bone modification in temperate settings, "corrosion of articular eminences" was observed on a number of bones left in permanently subaqueous or humid, heavily vegetated conditions, with no signs of surface weathering elsewhere on the elements (Andrews and Cook, 1985, p. 679; Andrews, 1995, p. 149). This modification has also been observed on bone epiphyses and on cancellous bones buried in waterlogged sediment for extended periods of time (Andrews and Ersoy, 1990). However, when this modification occurred in subterranean conditions, corroded flakes were found next to the original bone in the adjacent sediment, and occasionally, articulated tooth rows were found in position adjacent to corroded mandibles (Andrews and Ersoy, 1990). Since corroded bone flakes were not found adjacent to any bones subject to inferred “wet rot,” this suggests most of this alteration occured prior to ultimate burial. Recent observation of this inferred “wet rot” has been noted in other dinosaur bonebeds (Roberts, 2005), and was described to be almost identical to the epiphyseal corrosion on elements in the SRB (Roberts, personal comm.).

CHAPTER 8

DISCUSSION

The SRB is an accumulation of juvenile lambeosaur bones, with elements showing a very low degree of weathering, a moderate frequency of abrasion with existing abrasion predominantly moderate in extent, moderate fracturing with existing fractures restricted to styles representative of fresh breaks, near-complete disarticulation, selective removal of smaller, lighter elements, and inferred “wet rot” common to epiphyses and occasionally other spongy bone.

The bonebed was deposited as a massive, normally graded, clast-supported to matrix-supported conglomerate of bone and calcareous clasts in a matrix of silty mud and very fine- to medium-grained sand. Elongate elements in the deposit show a preferred orientation in trend, but random plunge. The bonebed overlies a massive sandstone, with a sharp, bioturbated contact separating the two beds. Elements at the base of the bonebed occasionally protrude into the underlying sandstone.

SRB Deposition and Comparison to other Two Medicine Bonebeds

Many features of the SRB are diagnostic of its mode of deposition: very poor sorting (clay - sand - 0.5 m bone), normal grading, presence of organics, large clasts floating in a fine-grained matrix, preferred orientation and steep plunge of elongate elements (clasts), and a massive structure with no signs of internal stratification, bioturbation, or pedogenic alteration. Collectively, these are all features typical of modern and ancient debris flow deposits (Crandell, 1971; Mills, 1984; Shultz, 1984; Pierson and Scott, 1985; G. A. Smith, 1986; Crandell, 1987; Scott, 1988; Meyer and Wells, 1997; Sohn et al., 1999; Capra and Macias, 2002; Malet et al., 2005), including deposits in which bones are the dominant clast component (Table 7; Andrews and Alpagut, 1990; Andrews and Ersoy, 1990; Rogers, 2005; Eberth et al., 2006; Lovelace, 2006).

Comparing the SRB to other bonebeds in the Two Medicine Formation supports this interpretation (Table 7). Dinosaur bonebeds in a matrix of fines (mudstone – siltstone) in the Two Medicine Formation are commonly attributed to four depositional modes (Table 7):

Autochtonous-paratochtonous lacustrine deposition: individual carcasses, introduced to small lakes without extensive prior fluvial transport, are interred under lacustrine sediment with little disturbance (Lambeosite, WHB, and JBS of Table 7). This depositional mode is insufficient to explain the SRB, as the SRB has no indication of aqueous conditions (varves, caliche horizons, aqueous invertebrates), near-complete disarticulation and disassociation, and moderate levels of fracturing (Varricchio and Horner, 1993; Varricchio, 1993).

Bioturbated watering hole accumulations: attritional carcass accumulations in and near water sources are heavily bioturbated, and buried via trampling and/or interred under sediment from subsequent flooding episodes (CBB, DRQ, WQ, and JBS of Table 7). Deposition in respective water sources is insufficient for SRB, for the lack of aqueous indicators listed above. Accumulation on adjacent floodplains is also insufficient, as the

Table 7: Taphonomic data for bonebeds from the Two Medicine Formation and other debris flow-hosted bonebeds (based on Varricchio and Horner, 1993).

Locality	Lambeosite[1]	WHB[1]	CBB[2]	DRQ[2]	WQ[1,2]	JBS[3]	BCN[1]
Formation				Two Medicine			
Matrix	Silty mudstone	Silty mudstone	Sandy siltstone	Sandy siltstone	Silty mudstone	Silty mudstone	Silty mudstone
Bonebed lithology	Not reported	Not reported	Massive, lenticular	Massive, lenticular	Massive, lenticular, root traces, caliche horizon	Massive, calcic, poorly sorted	Not reported
Dominant fauna	Monotaxic lambeosaurid	Monotaxic lambeosaurid	Monotaxic ceratopsid	Paucitaxic ceratopsid and hadrosaurid	Monotaxic hadrosaurid	Multitaxic vertebrata	Monotaxic lambeosaurid
Other fauna and flora	Rare semiaquatic vertebrates	Rare semiaquatic vertebrates	Abundant aquatic invertebrates and carbonized plant debris, rare semiaquatic vertebrates	Abundant aquatic invertebrates and carbonized plant debris, rare semiaquatic vertebrates	Rare terrestrial vertebrates	Abundant terrestrial and aquatic gastropods and coalified wood fragments	Rare terrestrial vertebrates
Bone density	$5/m^2$	$5/m^2$	$7/m^2$	$3/m^2$	$7/m^2$	$9/m^2$	$100/m^2$
Element representation	(Voorhies) Group I underrepresented	Group I underrepresented	Group I underrepresented	Group I underrepresented	Group I underrepresented	Equal representation	Equal representation
Association and articulation	Disarticulated to partial articulation	Disarticulated with some association	Disarticulated, disassociated	Disarticulated, disassociated	Disarticulated, disassociated	Disarticulated, commonly associated	Disarticulated to partial articulation
Bone orientation	No plunge, strong trend alignment	No plunge	No plunge, no trend alignment	No plunge, no trend alignment	Random plunge, no trend alignment	No plunge (lake) to steeply dipping (shore), weak trend alignment	No plunge, strong trend alignment
Vertical bone arrangement	Not reported	Not reported	Concentrated at base, ungraded	Concentrated at base, ungraded	Not reported	Concentrated at base	Not reported
Pre-diagenetic bone modification	Rare breakage and weathering	Rare breakage and weathering	Extensive breakage, differential weathering	Extensive breakage and weathering	Minor breakage	Rare (lake) to severe (shore) breakage, weathering, and abrasion	Rare breakage and weathering
Interpreted deposition	Lacustrine (small lake)	Possible lacustrine (small lake)	Watering hole accumulation	Watering hole accumulation	Watering hole accumulation	Lacustrine (shallow lake) and associated shore accumulation	Crevasse splay

Table 7: continued

Locality	Camposaur[1,4]	SRB	DWQ[5]	Jimbo Quarry[6]	Anembalemba[7]	Paşalar[8]
Formation	Two Medicine	Two Medicine	Cedar Mountain (Jr)	Morrison (Jr)	Maevarano (K)	Gönen Basin (Mio)
Matrix	Sandy mudstone	Sandy mudstone	Sandy mudstone	Mudstone	Sandy mudstone	Sandstone
Bonebed lithology	Massive, poorly sorted	Massive, poorly sorted	Massive, poorly sorted	Massive, poorly sorted	Massive, poorly sorted	Massive, poorly sorted
Dominant fauna	Monotaxic lambeosaurid	Monotaxic lambeosaurid	Multitaxic dinosaurid	Paucitaxic sauropod and theropod	Multitaxic vertebrata	Multitaxic mammalia
Other fauna and flora	Rare terrestrial vertebrates	Rare terrestrial and semiaquatic vertebrates	Rare semiaquatic vertebrates	Abundant coalified plant material	Rare gastropods, bivalves, and chonchostracans	Not reported
Bone density	$>10/m^2$	$>130/m^2$ (max)	$20/m^2$	Not reported	Unspecified, described as high	Not reported
Element representation	Group I underrepresented	Group I underrepresented	Not reported	Equal representation	Equal representation	Not reported
Association and articulation	Disarticulated, disassociated	Disarticulated, disassociated	Disarticulated	Disarticulated	Full articulation to disarticulated	Disarticulated
Bone orientation	No plunge, no trend alignment to strong alignment	Random plunge, significant trend alignment	Strong trend alignment	Strong trend orientation	Random trend and plunge orientation	No plunge, random trend orientation
Vertical bone sorting	Normal grading, clast- to matrix-supported	Normal grading, clast- to matrix-supported	Normal to inverse to ungraded, matrix-supported	Matrix-supported, ungraded	Not reported	Normal grading
Pre-diagenetic bone modification	Moderate abrasion, extensive breakage, clast interaction, unweathered	Minor weathering, moderate abrasion and breakage	Extensive breakage, significant weathering, scavenging marks	Extensive breakage, significant clast interaction	Differential weathering, feeding traces, extensive time averaging	Extreme breakage, abrasion, and weathering, scavenging marks
Interpreted deposition	Fluid debris flow	Cohesive debris flow	Debris flow	Debris flow	Debris flow	Debris flow

[1]Varrichio and Horner, 1993 (WHB = West Hadrosaur Bonebed, BCN = Blacktail Creek North)
[2]Rogers et al, 1990 (CBB = Canyon Bone Bed, DRQ = Dino Ridge Quarry, WQ = West Side Quarry)
[3]Varricchio, 1995 (JBS = Jack's Birthday Site)
[4]Schmitt et al, 1998
[5]Eberth et al, 2006; Britt et al, 2006 (DWQ = Dalton Wells Quarry)
[6]Lovelace, 2006
[7]Rogers, 2005
[8]Andrews and Alpagut, 1990; Andrews and Ersoy, 1990

bioturbation commonly results in extensive fracturing and scratching of bone, and no trend alignment of elongate elements (Rogers, 1990; Varricchio, 1995). The consistency of the matrix in the SRB also argues against burial under cumulative flood-deposited sediment.

Additionally, studies of modern watering hole accumulations known to be subject to trampling are inconsistent with the SRB assemblage. While trampling can result in usually high numbers of elongate elements with steep plunge (Hill and Walker, 1972; Haynes, 1983a; Fiorillo, 1988a), modern trampled bonebeds are commonly dominated by splintered and crushed fragile elements (ribs, scapulae, vertebrae; Gifford, 1976; Haynes, 1983a), often with more than 50% of elongate elements exhibiting fractures (Haynes, 1983a), and exhibiting extensive striations, scrapes, and scratches (Andrews and Cook, 1985). Trampling of elements into sediment also appears to be a weak process in modern bonebeds, with the majority of elements still exposed at the surface (Gifford, 1976; Haynes, 1983a), and only small, dense bones being driven into the substrate (podials and phalanges; Gifford, 1976).

Crevasse splay deposition: carcasses are entrained in a crevasse splay during an overbank flood (BCN of Table 7). This depositional mode is insufficient for the SRB, considering the predominance of fines in the matrix, and the absence of any indication of turbulent flow.

Debris flow deposition: carcasses are entrained in a debris flow (Camposaur of Table 7). For the reasons listed above, this is the most likely mode of deposition for the SRB. In addition, the SRB share similarities with Camposaur bonebed that are rare or unique among other Two Medicine bonebeds, including normal grading of bone and rock clasts, poor sorting of the bonebed sediment, and trend alignment of long bones in the absence of fluid flow (Varricchio and Horner, 1993; Schmitt et al.,1998). The SRB is interpreted to have been ultimately emplaced as a debris flow deposit.

Debris flows (hereafter defined as a sediment gravity flow in which sediment concentration exceeds 75 wt% or 50 vol%; see Costa, 1988; Gani, 2004), are subdivided into cohesive and non-cohesive debris flows by abundance of clay the matrix (measured as a dimensionless percent in relation to all other coarser sediment in the bed). A division at 10% clay is common (Crandell, 1971; Shultz, 1984; Pierson and Scott, 1985; Crandell, 1987; Scott, 1988; Coussot and Meunier, 1996; Meyer and Wells, 1997); visual examination of the matrix of the SRB showed a maximum of 20% sand. The matrix was not examined further to determine ratios of silt and clay, but it is unlikely that the remaining ~80% of matrix contained less than 10% clay; this suggests the SRB was entrained and deposited in a cohesive debris flow.

The examination of the matrix also excluded the possibility that the SRB was the deposit of a hyperconcentrated flow, which can resemble non-cohesive debris flows in restricted exposures (see Pierson and Scott, 1985; G. A. Smith, 1986; Meyer and Wells, 1997). Hyperconcentrated flows are characterized by a very sandy matrix, with even less clay than the matrix of non-cohesive debris flows (Pierson and Scott, 1985; Meyer and Wells, 1997; G. A. Smith, 1986; Sohn et al., 1999). In addition, the SRB possesses no features indicative of the turbulent flow common to hyperconcentrated flow deposits, including bipartite clast deposition (Gani, 2004), a scoured base or undulating upper surface (Sohn et al.,1999), faint stratification (Pierson and Scott, 1985; G. A. Smith, 1986), or clast imbrication (Meyer and Wells, 1989).

Debris Flow Genesis

There are numerous initiations for debris flows; all that is required is the presence of "a large volume of loose rock debris and water to mobilize it" (Crandell, 1987, p. 11), and a slope which need not be steeper than 1 - 2% (Rodine and Johnson, 1976). Possible causes include:

1) Volcanically-induced runoff (melting of snow or ice, undamming of crater lakes) or avalanche (syn-eruption debris)
2) Intense rainfall on loose debris and/or steep terraine
3) Seismically-induced debris avalanche or undamming of lakes/ponds
4) Bank collapse in fluvial channels
5) Rapidly increased runoff in fluvial systems
6) Subaqueous (lake/pond) slumping/sliding

Some of these scenarios can be quickly excluded. The absence of volcaniclastic material from the SRB sediment suggests the SRB debris flow wasn't initiated in a volcanic setting (1); additionally, volcaniclastic sediment commonly forms non-cohesive flows (Crandell, 1971; Pierson and Scott, 1985; Pierson, 1986; G. A. Smith, 1986; Crandell, 1987). Similarly, debris flows initiated by bank collapse (4) are commonly dominated by sand, with seldom more than 10% fines (silt and clay; Martin and Turner, 1998).

Catastrophic undamming of lake or ponds, whether volcanically induced (1) or seismically induced (3), would likely result in deposit with sediment containing aqueous indicators; as mentioned previously, none are present in the SRB, making such an origin unlikely. Similarly, the fact that the SRB overlies a sandstone with a sharp, bioturbated contact, and is overlain by mudrock with no aqueous fossils or laminations, and showing signs of pedogenesis, makes it doubtful that the SRB debris flow was subaqueous (6).

The SRB debris flow was probably not initiated by a debris avalanche (3). Debris avalanches transform into debris flows as the original avalanche sediment incorporates surface water (Martin and Turner, 1998; Malet et al., 2005). Deposits of such debris flows typically contain a large percentage of coarse, angular clasts from the initial avalanche material; the absence of angular non-bone clasts in the SRB suggests the flow was not initiated in this fashion.

Intense rainfall on hillslopes (2) can introduce enough water into pore space to initiate slumping, which can subsequently transform into debris flows (Malet et al., 2005; Gabet and Mudd, 2006). However, this transformation occurs through the infiltration of water into pore space (Malet et al., 2005); without sufficient sand content (as high as 50%), the pore space is insufficient to allow the transition to a debris flow (Gabet and Mudd, 2006). In addition, for sediment high in clay content, intense rainfall appears to be insufficient to initiate a debris flow – a combination of intense rainfall, thawing soil, and snowmelt is necessary (Malet et al., 2005). The climate of the Late Cretaceous of Western Montana was warm and seasonal, varying between a sub-humid to temperate season, and a semi-arid dry season (see Dodson, 1971; Varricchio, 1995); the low sand content in the SRB, and low likelihood of snow and frozen soil in the warm climate, suggest the SRB debris flow was probably not initiated by intense rainfall on loose sediment and/or steep terraine (2).

This leaves the possibility of increased sediment runoff into fluvial systems (5). Rarely, streamflows or flood flows transform into a debris flow if sufficient sediment is introduced (Malet et al., 2005), or when water is rapidly lost water when overriding permeable sediment (Bull, 1972). More common is the transformation into a debris flow through bulking, the incorporation of sediment by non-turbulent erosion ("scraping") at the flow boundary (Pierson and Scott, 1985; Scott, 1988; Lavigne and Suwa, 2004). Though bulking is most common to non-cohesive debris flows in volcanic settings (Crandell, 1971; Pierson and Scott, 1985; Pierson, 1986; Crandell, 1987; Scott, 1988; Best, 1992f; Capra and Macias, 2002), this process has also been proposed to initiate cohesive debris flows as well (Cannon et al., 1997; Meyer and Wells, 1997). While it may seem unlikely that a streamflow could bulk enough sediment to reach the necessary concentration of sediment (>75 wt%) of a debris flow, bulking factors of 400 – 600% have been documented (Capra and Macias, 2002). That the SRB was deposited in an overbank lends credence to this interpretation - bulking in a channel would erode coarse channels deposits; bulking in a floodplain would erode much finer sediment, resulting in a clay-rich debris flow deposited in an overbank environment, much like the SRB.

This type of debris flow initiation is likely if the original flood flow already contains significant sediment. Obtaining sufficient amounts of sediment often requires erosion throughout an entire drainage basin, possibly in combination with mass wasting directly into the fluvial system (Coussot and Meunier, 1996). Wildfire, which removes roots that anchor colluvium, and reduces evapotranspiration rates (=more rainfall infiltrating sediment), is commonly associated with such levels of erosion (Cannon et al., 1997; Meyer and Wells, 1997). The possibility that wildfire played a role in initiating the SRB debris flow is difficult to test – the presence of organics and plant material in the bonebed is suspect, unfortunately the only material large enough to examine was coalified, removing any evidence of its life history.

This interpreted debris flow initiation is also supported by the climate of the Late Cretaceous of Montana. Evidence for a seasonal climate includes growth rings in trees and *Champsosaurus* vertebrae (Dodson, 1971), color banding in mudrocks (red/grey bands in Fm overlying SRB) indicating repetitive pedogenic cycles (Platt and Keller, 1992), and the previously described indicators for both semi-arid and waterlogged exposure of SRB area strata. Inherent to such a seasonal climate would be intense, seasonal rainfall (Dodson, 1971; Rogers, 2005) which would lead to periods of intense erosion and runoff (Tunbridge, 1981).

In addition, the SRB debris flow appears to have been an individual, localized debris flow, in contrast to the repetitive, regional debris flow-hosted bonebeds of Rogers (2005) and Eberth et al. (2006). These regional-scale debris flows events left multiple, stacked bonebeds extending laterally for up to 40 m (Rogers, 2005; Eberth et al., 2006). The 2004 excavation didn’t expose bone extending farther than 5 – 6 m laterally from the quarry, though much of this may be due to modern erosion; earlier field work found bone extending only 5 – 6 m farther (Horner, personal comm.). In addition, the lack of any other debris flow deposits in the measured SRB area suggests the SRB debris flow was a localized occurrence.

The Debris Flow

The SRB is interpreted to have been deposited as a cohesive debris flow, initiated when intense seasonal rainfall produced a flood flow that incorporated fine-grained sediment through bulking as it flowed over a floodplain. Many of the lithologic features of the bonebed, and taphonomic feature of the bones, are interpreted to be direct results of the debris flow process.

The normal grading of the clasts (bones and calcareous clasts) in the SRB is interpreted to be a direct result of the debris flow. Normal grading results from incremental deposition of a laterally sorted debris flows, where an individual flow is segregated into separate, smaller “surges.” The flow head contains the largest clasts, and progressively smaller clasts are found farther back in the flow tail (Pierson, 1986, Fig. 13.6; Vallance and Scott, 1997); as this segregated debris flow is incrementally deposited, the coarsest clasts are deposited first, and as the flow overrides the initial deposit, flows of successively smaller clasts gradually build the deposit vertically (Major, 1997; Vallance and Scott, 1997; Major, 1998). While this process is more common among non-cohesive debris flows (Pierson, 1986; G. A. Smith, 1986), it has also been documented for cohesive debris flows (Vallance and Scott, 1997; see Sohn et al., 1999, p. 122). The high clay content in the SRB debris flow likely cushioned the largest bones (Rogers, 1990), preventing the extreme cataclasis common to the larger clasts in the flow head of non-cohesive debris flows (Johnson and Rodine, 1984). Incremental deposition was likely responsible for some or all of the winnowing of the assemblage as well - incremental deposition can bias an accumulation against smaller clasts, as the more distal, more fluid deposits containing the smallest clasts override the debris flow without deposition. In addition, the presence of normal grading also argues against the previously mentioned possibility of a watering hole accumulation. While trampling can certainly drive elements into sediment, it is highly unlikely that trampling can replicate the specific vertical distribution of normal grading (see Fig. 19).

It is uncertain at what point in the flow event the bones were incorporated into the flow. If they were present in the initial flood flow, the fluvial transport could account for some abrasion and winnowing, and possibly some fracturing. However, in bulked debris flows, the initial sediment in the flood flow is the fine-grained portion, and larger clasts are incorporated later (Meyer and Wells, 1997).

At the time of writing, there is an absence of empirical data on bone clasts transported in debris flows, but it is likely that some of the abrasion and fracturing were a result of debris flow transport. Trampling of elements into a sandy substrate can result in "low grade" abrasion (Brain, 1967) – it is plausible that laminar flow in a matrix of fines and sand could also produce minor abrasion. Cataclasis is a common in debris flows, even in cohesive flows (Vallance and Scott, 1997; Eberth et al.,2006) In fact, the debris flow-hosted bonebed of Lovelace (2006), which was likely cohesive, showed evidence of significant clast interaction, including bones lithified in the process of damaging each other. This clast interaction could account for a large portion of fractured elements in the

SRB, especially elements showing fractures similar to percussion marks (Fig. 32) and fractured elements with the fractured portions still in close proximity (Figs. 34, 35; Lovelace, 2006).

The near-complete disarticulation and disassociation of the assemblage could also have been a result of debris flow transport. Given the possibility of cataclasis, it is plausible that this process could have at least disassociated, and probably disarticulated, many elements.

The trend and plunge of elongate elements in unusual. Clasts in clast-supported debris flow deposits commonly show a preferred trend and plunge, but this is almost exclusively confined to the flow margins, especially the flow front (Middleton, 1966; Mills, 1984; Major, 1988). The small volume of the SRB excavated could represent only a flow margin, but this does not explain the random plunge orientation. However, this feature could illustrate a difference between bone clasts and rock clasts, as preferred trend orientation (Eberth et al., 2006) and random plunge orientation (Andrews and Ersoy, 1990) of elongate elements is found throughout the vertical column in other debris flow-hosted bonebeds. Occassional parallel alignment of smaller elongate elements on opposing sides of larger elements (Fig. 27) is interpreted to be elongate elements of similar trend settling in association by chance, rather than an influence of larger elements on the flow of smaller.

The calcareous clasts, like the elements, are interpreted to be clasts incorporated during bulking. They show no evidence of having formed as nodules within the bonebed, showing no nucleation sites (Nadon, 1994), no incorporated “floating” clastic grains from the matrix (Eberth and Miall, 1991), do not preferentially encase bone (Eberth et al., 2006), and are subrounded to rounded in shape (Lorenz, 1981). In addition, the calcareous clasts are part of the clast-supported framework in the lower depths of the bed, often in contact with several bones. The apparent contrast between the subrounded to rounded calcareous clasts and predominantly unabraded bones may not be problematic. It is unknown when the calcareous clasts were incorporated into the debris flow relative to the bones; the latter could have been incorporated much earlier, and subject to much more abrasion and cataclasis, or the calcareous clasts could have already been significantly rounded when entrained.

The fragmentary plant material found near the top of the SRB was likely incorporated along with bulked sediment, and was ultimately deposited near the surface of the flow (Meyer and Wells, 1997). The larger coalified plant fossils at the surface of the bed were probably not part of the debris flow, as they are found at the contact with the overlying mudrock and are parallel to the bedding plane.

The SRB debris flow was ultimately emplaced when its yield strength exceeded its flow velocity, either through continued bulking of sediment, loss of interstitial water, increased slope, decreased momentum, or a combination these factors. This can occur through absence of surface water (vs overriding rainfall or streamflow; Capra and Macias, 2002; Lavigne and Suwa, 2004; Malet et al., 2005), or through bulking of sufficient coarse sediment to result in water lost through increased pore space (Malet et al., 2005).

The sandstone on which the SRB debris flow was deposited was likely still partially moist when the bonebed was deposited, as evidence by the extrusion of some bones into the sandstone (Lovelace, 2006). The retention of the intricate bioturbated upper surface of the sandstone is not problematic – debris flows can pass over material as delicate as ash (Vallance and Scott, 1997), loose sand and leaves (Crandell, 1971), and duff (Scott, 1988; Meyer and Wells, 1997) with no signs of disruption.

The SRB debris flow probably stayed waterlogged for at least several days following deposition, as is common for debris flow deposits (Pierson and Scott, 1985). This would have allowed for the formation of the goethite nodules and drab green-grey color of the sediment (Retallack, 1997; written comm.), and could have caused some of the "wet rot" (Andrews and Ersoy, 1990). The gradational contact with the overlying mudrock suggests the SRB sediment was still moist when the subsequent fines were deposited.

Carcass Exposure

The interpretation of debris flow deposition only accounts for the ultimate emplacement of the SRB. Prior to transport in a debris flow, the assemblage could have experienced bioturbation or prior transport. This period of exposure likely wasn't extensive; the weathering stages indicate a maximum of two years exposure, and the lack of tooth marks suggests brief exposure as well.

Many of the bone modifications – abrasion, fracturing, disarticulation, "wet rot" – are at least partially taphonomic effects of the debris flow. However, this does not exclude a portion of these modifications from having occurred during prior exposure. Fracturing, in particular, probably occurred soon after death, given the predominance of fractures (spiral and transverse) indicating breaking of fresh bone, and a minority of fractures typical of trampling, such as fracturing of the edges of flat, thin elements (Gifford, 1984). The inferred "wet rot," if it occurred during exposure, indicates the presence of water, either in a humid, sheltered environment or as standing water (Andrews and Cook, 1985; Andrews, 1995).

Cause of Death

The SRB is an accumulation representing several individuals with elements sharing similar levels of weathering and other bone modification. These are factors characteristic of mass death assemblages, defined as a circumscribed area where a group of individuals die over a brief (hours to months) time span due to a single, uninterrupted agency of death (Haynes, 1988).

Carpenter (1988) established three forms of mortality responsible for mass death assemblages of terrestrial vertebrates: catastrophic mass mortality (CMM), noncatastrophic mass mortality (NCMM), and attritional mortality (AM). The dominance of one taxa and uniform preservation in the SRB indicates it is not the result of attritional mortality (Carpenter, 1988). Whether SRB is representative of catastrophic mass mortality or noncatastrophic mass mortality is uncertain; the dominance of one taxa is characteristic of noncatastrophic mass mortality, while the uniformity of weathering (or lack thereof) is more common among catastrophic mass mortality (Carpenter, 1988).

Several specific causes of mass mortality are consistent with the SRB, but none are favored. The most commonly interpreted cause of death in the Two Medicine is drought (Rogers, 1991; Varricchio and Horner, 1993; Varricchio, 1995), which can produce bonebeds in two distinct fashions (Norman, 1987). Widespread drought kills commonly result in attritional, multispecific accumulations; the SRB is more similar to localized droughts that produce noncatastrophic death assemblages (Norman, 1987), which can be less taxonomically diverse and selective toward younger individuals (Berger, 1983).

Mass drowning has also been proposed for dinosaur bonebeds, particularly for ceratopsian accumulations in the Campanian Dinosaur Park Formation to the north (Currie, 1981; Currie and Dodson, 1984; Visser, 1986; Sampson and Ryan, 1997; Ryan et al., 2001), but also for hadrosaurid accumulations in the Judith River Formation (Fiorillo, 1991). Deposits from mass drowning commonly exhibit a larger age range and more diverse taxa than that in SRB, but a number of ceratopsian bonebeds in the Dinosaur Park Formation, recently interpreted to be representative of mass drownings, are mono- to paucispecific and restricted in age class (Eberth and Getty, 2005).

Paleobiologic Implications

The interpretation of debris flow deposition makes the taxonomic bias of the SRB particularly significant. Bonebeds which are subject to debris flow transport (Andrews and Alpagut, 1990; Eberth et al.,2006) commonly incorporate allochtonous material and show high taphonomic and taxonomic diversity (Table 7). And while hadrosaurid bonebeds with predominantly juvenile age class representation are not uncommon in the Two Medicine (Varricchio and Horner, 1993), in all but one of these bonebeds, at least one adult specimen is present (Varricchio and Horner, 1993). Blacktail Creek North is the only other bonebed with no adult material, although this bonebed is dominated instead by nestling individuals (Varricchio and Horner, 1993). No adult material was obtained from the SRB, despite MNI values similar to, and NISP values greater than, other Two Medicine bonebeds (Varricchio and Horner, 1993). This is unlikely to be result of sorting, as smaller elements from adults and larger elements from younger individuals would have the same transport potential as juvenile elements (see Varricchio and Horner, 1993). Given the relatively small volume of the SRB excavated, it is possible that the excavated portion in a sample of an assemblage with a broader age range, much like West Hadrosaur Bonebed (Varricchio and Horner, 1993). However, given the quantity of elements excavated, this seems unlikely as well.

The dominance of the SRB by one age class of one taxa ultimately suggests either an original assemblage equally dominated by juvenile lambeosaurs, or an especially novel and unknown sorting factor in transport. This age class bias is probably most significant in its further support of the hypothesized herding/gregarious behavior of hadrosaurids (Horner and Makela, 1979; Horner, 1982; Rogers, 1991; Fiorillo, 1991; Horner, 2000), along with other related hypotheses of age segregation, seasonal reproduction, or high mortality of young (Varricchio and Horner, 1993). In fact, mass death assemblages from herding species are occassionally biased toward juveniles (Norman, 1987).

CHAPTER 9

SUMMARY AND CONCLUSIONS

The Sun River Bonebed is an assemblage of juvenile lambeosaur material in the Campanian Upper Two Medicine Formation of Montana. The bonebed is found in a stratigraphic succession interpreted to represent channel and overbank deposition from an ephemeral stream. The bonebed is a 45 cm thick conglomerate of bone and calcareous clasts in a matrix of silty green mud and sand. The conglomerate ranges from clast-supported at the base to matrix-supported at the surface, with clasts showing normal grading. Abundant fragmentary plant material is found in the upper 10 cm of the bonebed, coalified plant fossils are found at the contact with the overlying mudrock (Fm), and orange-brown zones (probably goethtite) are found throughout the vertical column. The bonebed overlies a medium to coarse grained massive sandstone (Sm) with a sharp, bioturbated contact, and grades into an overlying brown, calcareous silty mudstone (Fm) with abundant fragmentary plant material.

Material collected from the SRB is representative of a MNI of 8, based on the number of left dentaries. The SRB is highly skewed toward lambeosaur elements, with less than 2% of identifiable specimens assigned to other taxa, and the lambeosaur elements are highly skewed toward a late juvenile age class, with only one element of inconsistent size. Collected elements are characterized by a lack of weathering, a moderate frequency of abrasion, spiral and transverse fractures, and inferred “wet rot” to the epiphyses. Tooth marks are rare in the assemblage.

Elements are almost exclusively disarticulated, with no signs of association. Elongate bones show a preferred trend orientation, but random plunge. Large, dense bones are overrepresented in the assemblage, with smaller, less dense bones underrepresented.

The SRB is interpreted to represent an accumulation with a multi-stage taphonomic history, with four major stages:

1) A mass mortality event of juvenile lambeosaurs, with drought kill and mass drowning both plausible causes. This resulted in an initial assemblage dominated by one age class within one taxa.

2) Exposure of the carcasses to bioturbation/trampling and possible transport, resulting in one or more of the following: weathering, disarticulation, fracturing of fresh bone, abrasion, and inferred "wet rot."

3) Incorporation with calcareous clasts into a cohesive debris flow, likely initiated through the bulking of a flood flow moving over a floodplain. This produced a poorly-sorted, normally graded assemblage in a clay-rich matrix, and resulted in trend orientation, random plunge, and additional fracturing, abrasion, and disarticulation.

4) Emplacement on a crevasse channel sandstone in a waterlogged condition, followed by burial under successive floodplain fines. The waterlogged condition of the sediment resulted in the formation of possible goethite nodules, and possibly additional "wet rot."

The restricted taxic representation and age class of the SRB lends support to many of the paleobiologic interpretations of hadrosaurids, including age segregation, seasonal reproduction, and herding behavior.

REFERENCES CITED

Abler, W.L. 1984. A three-dimensional map of a paleontological quarry. Contributions to Geology, University of Wyoming 23 (1): 9-14.

Agenbroad, L.D. 1984. Hot Springs, South Dakota: entrapment and taphonomy of Columbian Mammoth. *In* Martin, P.S., and R.G. Klein, eds, Quaternary Extinctions: A Prehistoric Revolution, Tucson, University or Arizona, pp. 113-127.

Allen, J.R.L. 1977. The possible mechanics of convolute lamination in graded sand beds. Journal of the Geological Society of London 134: 19-32.

Allmendinger, R.W. 2002. Stereonet for Windows v 1.1, Cornell University, Ithaca, NY: www.geo.cornell.edu/geology/faculty/RWA/maintext.html

Alonso-Zarza, A.M., and P.G. Silva. 2002. Quaternary laminar calcretes with bee nests: evidence of small-scale climatic fluctuations, Eastern Canary Islands, Spain. Palaeogeography, Palaeoclimatology, Palaeoecology 178: 119-135.

Andrews, P. 1995. Experiments in taphonomy. Journal of Archaeological Science 22: 147-153.

Andrews, P., and B. Alpagut. 1990. Description of the fossiliferous units at Paşalar, Turkey. Journal of Human Evolution 19: 343 – 361.

Andrews, P., and J. Cook. 1985. Natural Modifications to bones in a temperate setting. Man (N.S.) 20: 675-691.

Andrews, P., and A. Ersoy. 1990. Taphonomy of the Miocene bone accumulations at Paşalar, Turkey. Journal of Human Evolution 19: 379-396.

Behrensmeyer, A.K. 1978. Taphonomic and ecologic information from bone weathering. Paleobiology 4 (2): 150-162.

Behrensmeyer, A.K., and R.W. Hook. 1992. Paleoenvironmental contexts and taphonomic modes. *In* A.K. Behrensmeyer, J.D. Damuth, W.A. DiMichele, R. Potts, H.D. Sues, and S.L. Wings (eds.). Terrestrial Ecosystems through Time, Evolutionary Paleoecology of Terrestrial Plants and Animals. Chicago, University of Chicago, pp. 15-136.

Berger, J. 1983. Ecology and catastrophic mortality in wild horses: implications for interpreting fossil assemblages. Science 220: 1403-1404.

Berger, J., S. Dulamstseren, S. Cain, D. Enkkhbileg, P. Lichtman, Z. Namshir, G. Wingard, and R. Reading. 2001. Back-casting sociality in extinct species: new perspectives using mass death assemblages and sex ratios. Proceedings of the Royal Society of London B 268: 131-139.

Best, J.L. 1992. Sedimentology and event timing of a catastrophic volcaniclastic mass flow, Volcan Hudson, Southern Chile. Bulletin of Volcanology 54: 299 – 318.

Blumenschine, R.J. 1986. Carcass consumption sequences and the archaeological distinction of scavenging and hunting. Journal of Human Evolution 15: 639-659.

Blumenschine, R.J., and C.W. Marean. 1993. A carnivore’s view of archaeological bone assemblages. *In* J. Hudson (ed.). From Bones to Behavior: Ethnoarcheological and Experimental Contributions to the Interpretation of Faunal Remains, Center for Archaeological Investigations, Occassional Paper No. 21. Southern Illinois University, pp. 273-300.

Brain, C.K. 1967. Bone weathering and the problem of bone pseudo-tools. South African Journal of Science 63: 97-99.

Brierley, G.J. 1996. Channel morphology and elements assemblages: a constructivist approach to facies modeling. *In* P.A. Carling, and M.R. Dawon (eds.). Advances in Fluvial Dynamics and Stratigraphy. John Wiley & Sons, Chichester, pp. 265-298.

Briggs, D.E.G., P.R. Wilby, B.P. Pérez-Moreno, J.L. Sanz, and M. Fregenal-Martínez. 1997. The mineralization of dinosaur soft tissue in the Lower Cretaceous of Las Hoyas, Spain. Journal of the Geological Society 154: 587-588.

Britt, B.B., R.D. Scheetz, D.B. Brinkman, and D.A. Eberth. 2006. A Barremian Neochoristodere from the Cedar Mountain Formation, Utah, U.S.A.. Journal of Vertebrate Paleontology 26 (4): 1005-1008.

Bull, W.B. 1972. Recognition of alluvial fan deposits in the stratigraphic record. *In* J.K. Rigby, and W.K. Hamblin (eds.). Recognition of ancient sedimentary environments: SEPM Special Publication 16: 63-83.

Cannon, S.H., R.M. Kirkham, and M. Parise. 2001. Wildfire-related debris-flow initiation processes, Storm King Mountain, Colorado. Geomorphology 39: 171 – 188.

Capra, L., and J.L. Macías. 2002. The cohesive Naranjo debris-flow deposit (10 km^3): a dam breakout flow derived from the Pleistocene debris-avalanche deposit of Nevado de Colima Volcano (México). Journal of Volcanology and Geothermal Research 117: 213-235.

Carpenter, K. 1988. Dinosaur bone beds and mass mortality. Implications for the Cretaceous-Tertiary extinction, LPI contribution, no. 673: 24-26.

Channing, A., M.H. Schweitzer, J.R. Horner, and T. McEneaney. 2004. A silicified bird from Quaternary hot spring deposits. Proceedings of the Royal Society of London B 272: 905-911.

Chin, K., T.T. Tokaryk, G.M. Erickson, and L.C. Calk. 1998. A king-sized theropod coprolite. Nature 393: 680-682.

Collinson, J.D., and D.B. Thompson. 1982. Sedimentary structures. London, George Allen & Unwin, 437 p.

Collinson, J.D. 1969. The sedimentology of the Grindslow Shales and Kinderscout Grit: a deltaic complex in the Namurian of Northern England. Journal of Sedimentary Petrology 39: 194-221.

Costa, J.E. 1988. Rheologic, geomorphic, and sedimentologic differentiation of water flood, hyperconcentrated flows, and debris flows. *In* V.R. Baker, R.C. Kochel, and P.C. Patton (eds.). Flood Geomorphology. John Wiley and Sons, New York, pp. 113-122.

Coussot, P., and M. Meunier. 1996. Recognition, classification, and mechanical description of debris flows. Earth-Science Reviews 40: 209-227

Crandell, D.R. 1971. Postglacial lahars from Mount Rainier volcano, Washington. U.S. Geol. Surv. Prof. Paper 677: 75 p.

Crandell, D.R. 1987. Deposits of pre-1980 pyroclastic flows and lahars from Mount St. Helens volcano, Washington. U.S. Geol. Surv. Prof. Paper 1444: 94 p.

Currie, P.J. 1981. Hunting dinosaurs in Alberta’s great bonebed. Canadian Geographic 101 (4): 35-39.

Currie, P.J., and P. Dodson. 1984. Mass death of a herd of ceratopsian dinosaurs. *In* W.E. Weif, and F. Westphal (eds.). Third Symposium on Mesozoic Terrestrial Ecosystems, Tübingen, Attempto Verlag: 61-66.

Davis, L.B, J.W. Fisher, Jr, M.C. Wilson, S.A. Chomko, and R.F. Morlan. 2000. Avonlea Phase winter fare at Lost Terrace, Upper Missouri River Valley of Montana: the vertebrate fauna. Plains Anthropologist 45 (174) Memoir 33: 53-69.

DeCelles, P.G. 1986. Sedimentation in a tectonically partitioned, nonmarine foreland basin: the Lower Cretaceous Kootenai Formation, Southwestern Montana. Geological Society of America Bulletin 97: 911-931.

Dodson, P. 1971. Sedimentology and taphonomy of the Oldman Formation (Campanian), Dinosaur Provincial Park, Alberta (Canada). Palaeogeography, Palaeoclimatology, Palaeoecology 10: 21-74.

Eberth, D.A. 1993. Depositional environments and facies transitions of dinosaur-bearing Upper Cretaceous redbeds at Bayan Mandahu (Inner Mongolia, People's Republic of China). Canadian Journal of Earth Science 31: 2196-2213.

Eberth, D.A., and M.A. Getty. 2005. Ceratopsian bonebeds: occurrence, origins, and significance. *In* P.J. Currie and E.B. Koppelhus (eds.). Dinosaur Provincial Park: A Spectacular Ancient Ecosystem Revealed, Indiana University Press: pp. 501-536.

Eberth, D.A., and A.D. Miall. 1991. Stratigraphy, sedimentology and evolution of a vertebrate-bearing, braided to anastomosed system, Cutler Formation (Permian-Pennsylvanian), north-central New Mexico. Sedimentary Geology 72: 225-252.

Eberth, D.A., D.S. Berman, S.S. Sumida, and H. Hopf. 2000. Lower Permian Terrestrial Paleoenvironments and vertebrate paleoecology of the Tambach Basin (Thuringia, Central Germany): the upland holy grail. Palaios 15: 293-313.

Eberth, D.A., B.B. Britt, R. Scheetz, K.L. Stadtman, and D.B. Brinkman. 2006. Dalton Wells: geology and significance of debris-flow-hosted dinosaur bonebeds in the Cedar Mountain Formation (lower cretaceous) of eastern Utah, USA. Palaeogeography, Palaeoclimatology, Palaeoecology 236: 217-245.

Falcon-Lang, H.J. 2003. Growth interruptions in silicified conifer woods from the Upper Cretaceous Two Medicine Formation, Montana, USA: implications for palaeoclimate and dinosaur palaeoecology. Palaeogeography, Palaeoclimatology, Palaeontology 199: 299-314.

Fedo, C.M., and J.D. Cooper. 1990. Braided fluvial to marine transition: the basal Lower Cambrian Wood Canyon Formation, southern Marble Mountains, Mojave Desert, California. Journal of Sedimentary Petrology 60: 220-234.

Fernandez-Jalvo, Y. 1988. Tafonomia de microvertebrados en Gran Dolina, Atapuerca (Burgos). Universidad Complutense, Madrid.

Fielding, C.R. 1984. Upper delta plain lacustrine and fluviolacustrine facies from the Westphalian of the Durham coalified, NE England. Sedimentology 32: 547-567.

Fiorillo, A.R. 1988a. A proposal for graphic presentation of orientation data from fossils. Contributions to Geology, University of Wyoming 27 (1): 1-4.

Fiorillo, A.R. 1988b. Taphonomy of Hazard Homestead Quarry (Ogallala Group), Hitchcock County, Nebraska. Contributions to Geology, University of Wyoming 27 (2): 57-97.

Fiorillo, A.R. 1991. Taphonomy and depositional setting of Careless Creek Quarry (Judith River Formation), Wheatland County, Montana, U.S.A.. Palaeogeography, Palaeoclimatology, Palaeoecology 81: 281-311.

Gabet, E.J., and S.M. Mudd. 2006. The mobilization of debris flows from shallow landslides. Geomorphology 74: 207-218.

Gani, M.R. 2004. From turbid to lucid: a straightforward approach to sediment gravity flows and their deposits. The Sedimentary Record 2 (3): 4-8.

Genise, J.F., M.G. Mángano, L.A. Buatois, J.H. Laza, and M. Verde. 2000. Insect trace fossil associations in paleosols: the *Coprinisphaera* ichnofacies. Palaios 15: 49-64.

Gifford, D.P. 1984. Taphonomic specimens, Lake Turkana. National Geographic Research Reports, 1976 Projects: 419-428.

Gill, J.R. and W.A. Coban. 1973. Stratigraphy and geologic history of the Montana Group and equivalent Rocks, Montana, Wyoming, and North and South Dakota. United States Geological Society Professional Paper 776: 38 p.

Harms, J.C. and R.K. Fahnestock. 1965. Stratification, bed forms, and flow phenomena (with an example from the Rio Grande). *In* G.V. Middleton (ed.). Primary Sedimentary Structures and their Hydrodynamic Interpretation, Society of Economic Paleontologists and Mineralogists Special Publication No. 12: 84-115.

Harms, J.C., J.B. Southard, D.R. Spearing, and R.G. Walker. 1975. Depositional environments as interpreted from primary sedimentary structures and stratification sequences. SEPM Short Course 2: 161 p.

Haynes, G. 1980. Evidence of carnivore gnawing on Pleistocene and Recent mammalian bones. Paleobiology 6 (3): 341-351.

Haynes, G. 1983a. Frequencies of spiral and green-bone fractures on ungulate limb bones in modern surface assemblages. American Antiquity 48 (1): 102-114.

Haynes, G. 1983b. A guide for differentiating mammalian carnivore taxa responsible for gnaw damage to herbivore limb bones. Paleobiology 9 (2): 164-172.

Haynes, G. 1988. Mass deaths and serial predation: comparative taphonomic studies of modern large mammal death sites. Journal of Archeoloical Sciences 15: 219-235.

Haszeldine, R.S. 1984. Muddy deltas in freshwater lakes, and tectonism in the Upper Carboniferous Coalfield of NE England. Sedimentology 32: 811-822.

Hill, A., and A. Walker. 1972. Procedures in vertebrate taphonomy; notes on a Uganda Miocene fossil Locality. Journal of the Geological Society of London 128: 399-406.

Horner, J.R. 1982. Evidence of colonial nesting and "site fidelity" among ornithischian dinosaurs. Nature 297: 675-676.

Horner, J.R. 1984. Three ecologically distinct vertebrate faunal communities from the Late Cretaceous Two Medicine Formation of Montana, with discussion of evolutionary pressures induced by interior seaway fluctuations. Montana Geological Society 1984 Field Conference: 299-303.

Horner, J.R. 2000. Dinosaur reproduction and parenting. Annual Reviews of Earth and Planetary Science 29: 19-45.

Horner, J.R., and P.J. Currie. 1994. Embryonic and neonatal morphology and ontogeny of a new species of Hypacrosaurus (Ornithischia, Lambeosauridae) from Montana and Alberta. *In* K. Carpenter, K.F. Hirsch, and J.R. Horner (eds.). Dinosaur eggs and babies, Cambridge University Press: pp. 312-336.

Horner, J.R., and R. Makela, 1979. Nest of juveniles provides evidence of family structure among dinosaurs. Nature 282: 296-298.

Horner, J.R., A.D. Ricqles, and K. Padian. 2000. Long bone history of the hadrosaurid dinosaur Maiasaura peeblesorum; growth dynamics and physiology based on an ontogenetic series of skeletal elements. Journal of Vertebrate Paleontology 20 (1): 115-129.

Horner, J.R., D.J. Varricchio, and M.B. Goodwin. 1992. Marine transgressions and the evolution of Cretaceous dinosaurs. Nature 358: 59-61.

Horner, J.R., D.B. Weishampel, and C.A. Forster. 2004. Hadrosauridae. *In* D.B. Weishampel, P. Dodson, and H. Osmólska (eds.). The Dinosauria, 2nd edition, University of California Press, Berkeley: pp. 438-463.

Jackson, R.G. II. 1978. Preliminary evaluation of lithofacies models for meandering alluvial streams. *In* A.D. Miall (ed.). Fluvial Sedimentology, Canadian Society of Petroleum Geologists, Memoir 5: pp. 543-576.

Johnson, A.M., and J.R. Rodine. 1984. Debris flow. *In* D. Brunsden, and D.B. Prior (ed.). Slope Instability, Wiley, New York: pp. 257-361.

Jones, B.G., and B.R. Rust. 1983. Massive sandstone facies in the Hawkesbury Sandstone, a Triassic fluvial deposit near Sydney, Australia. Journal of Sedimentary Petrology 53: 1249-1259.

Kauffman, E.G. 1977. Geological and biological overview; Western Interior Cretaceous Basin. Mountain Geologist 14 (3-4): 75-99.

Kirschbaum, M.A., and P.J. McCabe. 1992. Controls on the accumulation of coal and on the development of anastomosed fluvial systems in the Cretaceous Dakota Formation of southern Utah. Sedimentology 39: 581-598.

Larsen, D., and L.J. Crossey. 1996. Depositional environments and paleolimnology of an ancient caldera lake: Oligocene Creede Formation, Colorado. Geological Society of America Bulletin 108 (5): 526-544.

Larsen, D., and P.H. Nelson. 2000. Stratigraphy, correlation, depositional setting, and geophysical Characteristics of the Oligocene Snowshoe Mountain Tuff and Creede Formation in two cored Boreholes. *In* P.M. Bethke and R.L. Hay (eds.). Ancient Lake Creede: Its volcano-tectonic setting, history of sedimentation and relation to mineralization in the Creede Mining District, Boulder. Geological Society of America Special Paper 346: 159-178.

Lavigne, F., and H. Suwa. 2005. Contrasts between debris flows, hyperconcentrated flows and stream flows at a channel of Mount Semeru, East Java, Indonesia. Geomorphology 61: 41-58.

Leeder, M. 1999. Sedimentology and sedimentary basin; from turbulence to tectonics. Oxford, Blackwell Science, 592 p.

Lehman, T.M. 1982. A ceratopsian bone bed from the Aguja Formation (Upper Cretaceous) Big Bend National Park, Texas. M.S. Thesis, University of Texas at Austin: 210 p.

Lorenz, J.C. 1981. Sedimentary and tectonic history of the Two Medicine Formation, Late Cretaceous (Campanian), northwestern Montana. Ph.D. thesis, Princeton University: 215 p.

Lorenz, J.C., and W. Gavin. 1984. Geology of the Two Medicine Formation and the sedimentology of a dinosaur nesting ground. Montana Geological Society Field Guide: 175-186.

Lovelace, D.M. 2006. An Upper Jurassic Morrison Formation fire-induced debris flow: taphonomy and paleoenvironment of a sauropod (Sauropoda: Supersaurus vivianae) locality, East-Central Wyoming. *In* J.R. Foster and S.G. Luca (eds.). Paleontology and Geology of the Upper Jurassic Morrison Formation, New Mexico Museum of Natural History and Science Bulletin 36: 47-56.

Lyman, R.L. 1994. Vertebrate Taphonomy. Cambridge University Press, Cambridge, UK: 524 p.

Malet, J.-P., D. Laigle, A. Remaître, and O. Maquaire. 2005. Triggering conditions and mobility of debris flows associated to complex earthflows. Geomorphology 66: 215-235.

Major, J.J. 1997. Depositional processes in large-scale debris-flow experiments. The Journal of Geology 105: 345-366.

Major, J.J. 1998. Pebble orientation on large, experimental debris-flow deposits. Sedimentary Geology 117: 151-164.

Martin, C.A.L., and B.R. Turner. 1998. Origins of massive-type sandstones in braided river systems. Earth-Science Reviews 44: 15-38.

McCabe, P.J. 1977. Deep distributary channels and giant bedforms in the Upper Carboniferous of the Central Pennines, Northern England. Sedimentology 24: 274-290.

McKee, E.D., Crosby, E.J., and H.L. Berryhill. 1967. Flood deposits, Bijou Creek, Colorado, June 1965. Journal of Sedimentary Petrology 38: 829-851.

Melchor, R.N., Genise, J.F., and S.E. Miquel, 2002. Ichnology, sedimentology, and paleontology of Eocene calcareous paleosols from a palustrine sequence, Argentina. Palaios 17: 16-36.

Mellett, J.S. 1974. Scatalogical origin of microvertebrate fossil accumulations. Science 185: 349-350.

Meng, Q., J. Liu, D.J. Varricchio, T. Huang, and C. Gao. 2004. Parental care in an ornithischian dinosaur. Nature 43: 145.

Meyer, G.A., and S.G. Wells. 1997. Fire-related sedimentation events on alluvial fans, Yellowstone National Park, U.S.A.. Journal of Sedimentary Research 67 (5): 776-791.

Miall, A.D. 2006. The Geology of Fluvial Deposits: Sedimentary Facies, Basin Analysis, and Petroleum Geology, 4th ed. Springer-Verlag: 582 p.

Miall, A.D. 1977. A review of the braided-river depositional environment. Earth Science Reviews 13: 1-62.

Mills, H. H. 1984. Clast orientation in Mount St. Helens debris-flow deposits, North Fork Toutle River, Washington. Journal of Sedimentary Petrology 54 (2): 626-634.

Middleton, G.V. 1966. Experiments on density and turbidity currents: iii. deposition of sediment. Canadian Journal of Earth Sciences 4: 475-505.

Morlan, R.E. 1980. Taphonomy and archaeology in the upper Pleistocene of the northern Yukon Territory; a glimpse of the peopling of the new world. National Museum of Man Mercury Series, Archaeological Survey of Canada Paper 94, Ottowa: 398 p.

Mossop, G.D., and P.D. Flach. 1983. Deep channel sedimentation in the Lower Cretaceous McMurray Formation, Athabasca Oil Sands, Alberta. Sedimentology 30: 493-509.

Nadon, G.C. 1994. The genesis and recognition of anastomosed fluvial deposits: data from the St. Mary River Formation, Southwestern Alberta, Canada. Journal of Sedimentary Research B64 (4): 451-463.

Norman, D.B. 1987. A mass-accumulation of vertebrates from the Lower Cretaceous of Nehden (Sauerland), West Germany. Proceedings of the Royal Society of London B 230: 215-255.

Pierson, T.C. 1986. Flow behavior of channelized debris flows, Mount St. Helens, Washington. *In* A.D. Abrahams (ed.). Hillslope Processes. Boston, Allen & Unwin: p. 269-296.

Pierson, T.C., and K.M. Scott. 1985. Downstream dilution of a lahar: transition from debris flow to hyperconcentrated streamflow. Water Resources Research 21 (10): 1511-1524.

Platt, N.H., and B. Keller. 1992. Distal alluvial deposits in a foreland basin setting – the Lower Freshwater Molasse (Lower Miocene), Switzerland: sedimentology, architecture, and palaeosols. Sedimentology 39: 545-565.

Retallack G.J. 1997. Dinosaurs and dirt. *In* Wolberg, D.L., Stump, E., and G. Rosenberg, eds., Dinofest International: proceedings of a symposium held at Arizona State University. Academy of Natural Sciences, Philadelphia: pp. 345-359.

Roberts, E.M. 1999. Sedimentology, Taphonomy, and alluvial sequence stratigraphy of the lower Two Medicine Formation (Campanian) near Choteau, Montana. M.S. thesis, University of Montana: 66 p.

Roberts, E.M. 2005. Taphonomy of wet alluvial systems; a case example from the Cretaceous Western Interior Basin of Utah. Abstracts of papers, sixty-fifth annual meeting, Society of Vertebrate Paleontology, Journal of Vertebrate Paleontology 26 (3): 105.

Roberts, E.M., and M.S. Hendrix. 2000. Taphonomy of a petrified forest in the Two Medicine Formation (Campanian), Northwest Montana; implications for palinspastic restoration of the Boulder Batholith and Elkhorn Mountains volcanics. Palaios 15: 476-482.

Rodine, J.D., and A.M. Johnson. 1976. The ability of debris, heavily freighted with coarse clastic materials, to flow on gentle slopes. Sedimentology 23: 213-234.

Rogers, R.R. 1990. Taphonomy of three dinosaur bone beds in the Upper Cretaceous Two Medicine Formation of Northwestern Montana: evidence for drought-related mortality. Palaios 5: 394-413.

Rogers, R.R. 1993. Systematic patterns of time-averaging in the terrestrial vertebrate record: a Cretaceous case study. *In* S.M. Kidwell and A.K. Behrensmeyer (eds.). Taphonomic Approaches to Time Resolution in Fossil Assemblages, Paleontological Society, Short Courses in Paleontology, no. 6: pp. 228-249.

Rogers, R.R. 1998. Sequence analysis of the Upper Cretaceous Two Medicine and Judith River Formations, Montana: nonmarine responses to the Claggett and Bearpaw marine cycles. Journal of Sedimentary Research 68 (4): 615-631.

Rogers, R.R. 2005. Fine-grained debris flows and extraordinary vertebrate burials in the Late Cretaceous of Madagascar. Geology 33 (4): 297-300.

Rogers, R.R., and S.M. Kidwell. 2000. Associations of vertebrate skeletal concentrations and discontinuity surfaces in terrestrial and shallow marine records: a test in the Cretaceous of Montana. Journal of Geology 108: 131-154.

Rogers, R.R., C.C. Swisher, and J.R. Horner. 1993. $^{40}Ar/^{39}Ar$ age and correlation of the nonmarine Two Medicine Formation (Upper Cretaceous), northwestern Montana, U.S.A.. Canadian Journal of Earth Sciences 31: 1066-1075.

Rust, B.R., and B.G. Jones. 1987. The Hawkesbury Sandstone south of Sydney, Australia: Triassic analogue for the deposit of a large, braided river. Journal of Sedimentary Petrology 57: 222-233.

Ryan, M.J., A.P. Russell, D.A. Eberth, and P.J. Currie. 2001. The taphonomy of a Centrosaurus (Ornithischia, Certopsidae) bone bed from the Dinosaur Park Formation (upper Campanian), Alberta, Canada, with comments on cranial ontogeny. Palaios 16: 482-506.

Sampson, S.D., and M.J. Ryan. 1997. Variation. *In* P.J. Currie and K. Padian (eds.). Encyclopedia of Dinosaurs. San Diego, Academic Press: p. 773-780.

Schmitt, J.G., Horner, J.R., Laws, R.R., and F. Jackson. 1998. Debris-flow deposition of a hadrosaur-bearing bone bed, Upper Cretaceous Two Medicine Formation, Northwest Montana. Abstracts of papers; fifty-eighth annual meeting; Society of Vertebrate Paleontology, Journal of Vertebrate Paleontology 18 (3): 76.

Scott, A.C. 1978. Sedimentological and ecological control of Westphaliain B plant assemblages from West Yorkshire. Proceedings of the Yorkshire Geological Society 41: 461-508.

Scott, K.M. 1988. Origin, behavior, and sedimentology of lahars and lahar-runout flows in the Toutle-Cowlitz River System. U.S. Geol. Surv. Prof. Paper 1447-A: A1-A74.

Shelton, J.A. 2007. Application of sequence stratigraphy to the nonmarine upper Cretaceous Two Medicine Formation, Willow Creek Anticline, Northwestern Montana. M.S. Thesis, Montana State University – Bozeman: 238 p.

Shipman, P. 1981. Life history of a fossil, an introduction to taphonomy and paleoecology. Cambridge, Massachusetts, Harvard University Press: 222 p.

Shultz, A.W. 1984. Subaerial debris-flow deposition in the Upper Paleozoic Cutler Formation, Western Colorado. Journal of Sedimentary Petrology 54 (3): 759-772.

Slaughter, M., and J.W. Earley. 1965. Mineralogy and geological significance of the Mowry Bentonites, Wyoming. Special Paper, Geological Society of America, no. 83, 95 p.

Smith, D.G. 1986. Anastomosing river deposits, sedimentation rates and basin subsidence, Magdalena River, Northwestern Colombia, South America. Sedimentary Geology 46: 177-196.

Smith, G.A. 1986. Coarse-grained nonmarine volcaniclastic sediment: terminology and depositional process. Geological Society of America Bulletin 97: 1-10.

Smith, A.E. 1998. Volcanism and associated sedimentation in a retroarc foreland basin: the Upper Cretaceous Two Medicine Formation of West-Central Montana. M.S. Thesis, Montana State University, Bozeman: 170 p.

Smith, D.G., and N.D. Smith. 1980. Sedimentation in anastomosed river systems: examples from alluvial valleys near Banff, Alberta. Journal of Sedimentary Petrology 50 (1): 157-164.

Sohn, Y.K., Rhee, C.W., and B.C. Kim. 1999. Debris flow and hyperconcentrated flood-flow depositst in an alluvial fan, northwestern part of the Cretaceous Yongdong Basin, Central Korea. The Journal of Geology 107: 111-132.

Stear, W.M. 1985. Comparison of the bedform distribution and dynamics of modern and ancient sandy ephemeral flood deposits in the southwestern Karoo region, South Africa. Sedimentary Geology 45: 209-230.

Stock, C. 1956. Rancho La Brea: a record of Pleistocene life in California. Los Angeles County Museum of Natural History Science Series, no. 20, 6th edition.

Tunbridge, I.P. 1981. Sandy high-energy flood sedimentation – some criteria for recognition, with an example from the Devonian of S.W. England. Sedimentary Geology 29: 79-95.

Turner, B.R., and M. Munro. 1987. Channel formation and migration by mass-flow processes in the Lower Carboniferous fluviatile Fell Sandstone Group, northeast England. Sedimentology 35: 1107-1122.

Tye, R.S., and J.M Coleman. 1989. Depositional processes and stratigraphy of fluvially dominated lacustrine deltas; Mississippi delta plain. Journal of Sedimentary Petrology 59 (6): 973-996.

Vallance, J.W. and K.M. Scott. 1997. The Osceola mudflow and Mount Rainier: sedimentology and hazard implications of a huge clay-rich debris flow. Geological Society of America Bulletin 109: 143-163.

Varricchio, D.J. 1995. Taphonomy of Jack's Birthday Site, a diverse dinosaur bonebed from the Upper Cretaceous Two Medicine Formation of Montana. Palaeogeography, Palaeoclimatology, Palaeoecology 114: 297-323.

Varricchio, D.J., and J.R. Horner. 1993. Hadrosaurid and lambeosaurid bone beds from the Upper Cretaceous Two Medicine Formation of Montana: taphonomic and biologic implications. Canadian Journal of Earth Sciences 31: 997-1006.

Visser, J. 1986. Sedimentology and taphonomy of a Styracosaurus bonebed in the Late Cretaceous Judith River Formation, Dinosaur Provincial Park, Alberta. M.S. thesis, Univeristy of Calgary, Calgary, Alberta: 150 p.

Voorhies, M.R. 1969. Taphonomy and population dynamics of an early Pliocene vertebrate fauna, Knox County, Nebraska. Contributions to Geology, University of Wyoming, Special Paper No. 1: 68.

Voorhies, M.R. 1985. A Miocene rhinoceros herd buried in volcanic ash: National Geographic Society Research Reports 19: 671-688.

Walker, R.G., and D.J. Cant. 1984. Sandy Fluvial Systems. *In* R.G. Walker (ed.). Facies Models 2nd edition. Geoscience Canada Reprint Series 1: 71-89.

Woodward, L.A. 1981. Tectonic framework of Disturbed Belt of West-Central Montana: American Association of Petroleum Geologists Bulletin 65 (2): 291-302

APPENDICES

APPENDIX A:

BONEBED MAP OF THE SUN RIVER BONEBED

Appendix A: Bonebed map for the Sun River Bonebed, as seen parallel to bedding plane. Grey line indicates modern erosional surface, dashed red lines indicate 1 m grid boundaries.

APPENDIX B:

STRATIGRAPHIC SECTION OF THE SUN RIVER BONEBED AREA

Appendix B: Measured stratigraphic section for the Sun River Bonebed area. Thickness in cm to left of columns. Cumulative thickness at top of columns. Location of beds in figures to right of column.